MICROALGAL BIOFUELS:

Isochrysis sp. and *Phaeodactylum tricornutum*
lipid characterization and physiology studies

by

Tyler Jay Goepfert

Date and Place of Birth:
2 February 1980 in Williamsville, NY / USA

Submitted in partial fulfillment
of the requirements for the degree of

Master of Science
in the *Postgraduate Programme Renewable Energy*

Energy and Semiconductor Research Laboratory
Institute of Physics
Faculty of Mathematics & Science
Carl von Ossietzky University
Oldenburg / Germany

Day of Examination:	15th March 2010
1. Examiner:	Dr. Konrad Blum
2. Examiner:	Prof. Dr. Joachim Peinke
3. External advisor:	Dr. Mak Saito
4. External advisor:	Dr. Christopher Reddy

Dedication

*Completing this thesis is a milestone I would never have
achieved without the exceptional upbringing provided by my
parents; Ann and Ken Goepfert – I love you both very much –
for your encouragement, support, love, and devotion,
I dedicate this thesis to you.*

Certification

The undersigned certifies to have read and hereby recommends for acceptance by the University of Oldenburg a thesis entitled: "MICROALGAL BIOFUELS: *Isochrysis* sp. and *Phaeodactylum tricornutum* lipid characterization and physiology studies," in partial fulfillment of the requirements for the degree of Master of Science (Renewable Energy).

. . . . Dr. Konrad Blum (Supervisor)

. . . . Date (YYYY/MM/DD)

Declaration

I declare this thesis was prepared by me and that no means or sources have been used, except those which I have cited.

. . . . Tyler Jay Goepfert

. . . . Date (YYYY/MM/DD)

Acknowledgments

Abstract

Energy dense liquid fuels (e.g. No. 2 Fuel, Jet A, etc) are nearly indispensable within modern transport and energy supply infrastructure. With increasing environmental and geopolitical concerns related to petrochemicals and fuels, alternative biofuels are being sought. One promising feedstock can be derived via the microalgal solar energy conversion resource which does not compete with food supply, nor does it require fresh water (both already under strain in many regions). Despite the promise of many-fold increase in productivity relative to traditional terrestrial crops (oil-seeds, cellulosic biomass for ethanol, etc), microalga based fuels have many biological and technological aspects which must be better understood and improved. This thesis investigates the interface of biological dimensions and product fuel quality aspects (namely cloud-point and stability). It is shown that on account of unique hydrocarbon species (polyunsaturated long-chain alkenones, PULCAs), some marine prymnesiophytes (e.g. *Isochrysis* sp.) although promising in terms of bulk total lipid extract (TLE) may be undesirable for some biofuel end products (e.g. biodiesel). An alternative nitrogen source (urea) in the presence and absence of added nickel was investigated for growing the diatom *Phaeodactylum tricornutum*. During the batch culture experiments, daily or 2-day resolution sampling was performed for TLE, fatty acid methyl esters (FAMEs), nutrients (PO_4, Ni, NO_3+NO_2, NH_4, Si), biomass dry weights, protein expression, flow cytometry, and relative fluorescence (RFU). Significant results are presented here along with relevant environmental data (solar energy, photo-period, temperature). Results under these conditions are preliminary support and proof-of-concept for both technological and economic pilot-scale bioproduction of microalgal biofuels and other natural products (e.g. nutraceuticals, protein feeds, lubricants, etc). The FAME distribution and time-course changes under the treatment conditions are discussed with respect to nutrient depletion and the results have relevance to both biofuels and global biogeochemistry.

Keywords: renewable energy, microalgae, biofuel, biodiesel, biorefinery, industrial ecology, sustainability, climate change, oil, alkenone, CO_2, FAME, PULCA.

Contents

List of Figures

List of Tables

Chapter 1

Introduction

"Biofuels R&D is like the wild-west, there's a lot of hype and everybody is scrambling to get involved – what we need is for people to dig in and support or refute the hype with real-world proof of concept. One challenge seems to be going from laboratory flask to production scale."

- Mak Saito, Associate Scientist, WHOI; speaking in reference to grand potential of emerging science and applied efforts in biofuels – considerate of the hype and uncertainty present in microalgal biofuel prospects.

1.1 Aquatic Species Program, fossil oil, & geopolitical history

The Aquatic Species Program (ASP) was financed by the US government via the Department of Energy (DOE) for nearly two decades [96]. The aim of the ASP was to investigate the potential for energy production from cultivation of algae. It could be said that this program was one of the first serious investigations into potential of biomass energy inputs to the modern energy supply chain. Unlike other renewable energy resources, the substantial advantage of biomass is that solar energy is stored chemically and consequently an instantaneous consumer is not required to make use of the energy resource (as opposed to solar or wind technologies without storage infrastructure).

There will certainly be improvements in electric energy distribution and management (such as the "smart-grid" in discussion [59]), however our modern energy demand includes a larger indispensable fraction of non-electric power [2, Section 2, Figure 2.0]. While our surface transport may transition to non-petroleum sources such as all-electric battery or fuel cell technologies, modern aviation is unlikely to be sustained by any other portable storage than the energy dense jet fuels (e.g., Jet-A, ~43MJ/kg, [1]). Meanwhile, peak oil, is upon us or immanent according to a DOE sponsored report [41]. Unlike previous energy crisis we now have billions more people at the energy tap, not the least of which are citizens of China, India, and Indonesia amidst already far worse per capita energy intensive nations like Australia, Canada, and the USA.

The need exists for liquid fuels, and it is claimed that one source for sustainable supply could be microalgae [16, 44, 58] – avoiding many of the environmental concerns associated with other biomass energy crops (e.g., cellulosic ethanol as compared with biodiesel by *Hill et al.* [40]). Why then would the DOE discontinue the ASP? The answer to this question requires some history review. The ASP evolved out of DOE sponsored programs following concerns about energy security arising from the 1973 oil embargo (and related 1970s energy crisis) – following "economic recovery" the "apparent need" for alternative energy research dwindled (as did government funding).

Following the 1973 oil embargo and resulting geopolitical debacle including indirect but dubious transitions of both the US dollar and British pound sterling to fiat money (unbacked currency), business returned to "normal." Now we face growing environmental concerns (as presented by the IPCC since 1988 [47]), an economic crisis of global proportions, and a looming fossil energy decline [41]. The emerging picture is not one of sustainability, but conflict. Although funding for the ASP was cut in the 1990s with a final close-out report summarizing the findings [95], it has laid the foundation for renewed interest and offers hope for our future.

Our modern dependence on oil extends beyond combustion for heat and transport to include large-scale petrochemical generation such as fixed nitrogen via Haber-Bosch for agriculture. The energy return on investment for oil to date is so profound few other sources can compete as primary energy supplies to our growing and diverse end-uses. Like any living system our society has selected the easiest energy first. Yet a simple mass-balance would show that this is not a sustainable path. With more carbon dioxide (CO_2) in the atmosphere a trickle down effect is inevitable; as the oceans establish a new gas equilibrium state with CO_2, they become more acidic and the delicate pH balance behind many biogeochemical processes is shifted [22, 42].

Independent of our confidence in IPCC reports and what is at risk, the fact remains that oil is limited in supply and comes bundled with a plethora of geopolitical issues. Consequently a justified course would be to reincarnate the goals of the ASP. In the close-out report to the ASP it was stated,

> *"...[T]his report should be seen not as an ending, but as a beginning. When the time is right, we fully expect to see renewed interest in algae as a source of fuels and other chemicals. The highlights presented here should serve as a foundation for these future efforts."*

Indeed, the time may now be ripe for picking up where the ASP left off. This time however, relative oil costs are significantly improving economic viability [4]. Moreover, there have been substantial technology improvements in air-lift photobioreactors (PBR), automated system monitoring and control, and molecular tools (genomics, proteomics, metabolomics) [14, 15, 58, 65, 68, 110]. Optimism remains, despite more than a decade of abandon [61] and loosing priceless carefully screened cultures in that time [52]. The optimism in this theme is evident from both public and private investment into advanced research and commercialization of microalgal biofuels and co-products [21, 3, 73].

To continue, the principles of bioproduction, co-products, and biorefineries are important and shall be discussed next. As background to subsequent sections, this concise abstract by *Li et al.* [58] is quoted:

> *"Microalgae are a diverse group of prokaryotic and eukaryotic photosynthetic microorganisms that grow rapidly due to their simple structure. They can potentially be employed for the production of biofuels in an economically effective and environmentally sustainable manner. Microalgae have been investigated for the production of a number of different biofuels including biodiesel, bio-oil, biosyngas, and bio-hydrogen. The production of these biofuels can be coupled with flue gas CO_2 mitigation, wastewater treatment, and the production of high-value chemicals. Microalgal farming can also be carried out with seawater using marine microalgal species as the producers. Developments in microalgal cultivation and downstream processing (e.g., harvesting, drying, and thermochemical processing) are expected to further enhance the cost-effectiveness of the biofuel from microalgae strategy."*

It is helpful to know that three generations of plant-based feedstocks have come to be; *First Generation*: food-parts, from purpose grown crops, *Second Generation*: non-food-parts and/or waste from existing food agriculture (e.g., stalks and

stems from fruit harvest), and *Third Generation*: strictly non-food sources (e.g., algae, forestry residuals, others). Although these terms have gained popularity in biofuels discussion (e.g., *Gressel* [34]) they are not ideal because the successive generation terminology implies "improvements" which are ambiguous and indeed some aspects are even cause for concern as discussed by *Knothe* [54]. Nevertheless, downstream processing of crop products regardless of "generation" are a necessity and most effectively managed with the concept of a biorefinery as described next.

1.2 The biorefinery concept

Girisuta [33] provides a concise definition of biorefining as follows:

> *"Biorefining aims for a complete valorisation of the biomass source by performing the overall processes with a minimum loss of energy and mass and to maximize the overall value of the production chain. It consists of an efficient fractionation of the biomass into various value-added products and energy using physical separation processes in combination with (bio-) chemical and thermo-chemical conversion steps. In that sense, the biorefinery concept has similar objectives as today's petroleum refineries."*

Typically the biorefinery can have three main processes:

- Primary fractionation: separates biomass into it's six main components (cellulose, hemicellulose, lignin, proteins, amino acids, pure plant oil).

- Secondary fractionation: converts intermediate fractions to valuable end products (e.g., bio- fuels).

- Tirtiary processing: transforms the chemical intermediates to high added value end-products (e.g. via catalytic and or pyrolitic methods).

Residuals from the above processing and fractionation stages can be directed to heat and power generation via thermochemical conversion processes (e.g. direct combustion, gasification, pyrolysis).

1.3 Outlook for microalgal biofuels

Microalgae as a feedstock toward biofuel production has been shown to have superior advantages over traditional terrestrial crops in potential to satisfy transportation fuel needs at a defined cost-competitive relation dependent on the price of crude oil [16]. Indian researchers are screening indigenous microalgae strains hoping to seed and harvest them from simple and inexpensive open-pond systems as a feedstock for augmenting biofuel production [50]. Higher efficiency – though more expensive – closed uni-algal culture systems (PBRs) are successfully being employed by a number of private corporations for a wide range of products including fuels for surface vehicles as well as jet fuel [102].

Not all ventures are successful though – for example one headline reads: "The Harvard-MIT algae company winds down after spending millions and experiencing delays, technical difficulties."[1] Technical difficulties encountered by Green-Fuels might be a surprise, it was not inability to produce feedstock, but largely inability to harvest fast enough, that is, algae grew faster than they could be harvested. Where one venture is lost, another is born as the next (albeit more tentative) headline in this progression reads: "Rapidly growing algae and streamlined processes could mean $2 diesel by 2011 or 2012. But hurdles await."[2]

Media hype aside, in addition to the environmentally relevant need for carbon-neutral fuels, a wide variety of products can be made from microalgae (several being high-value products) [57]. Cyanobacteria were shown to be a source of many bioactive natural products by *Patterson et al.* [75]. In pharmaceuticals The biorefinery concept – to make use of all potential salable products – exploits the variety of products microalgae can produce. Bio-refinery concepts, economies of scale, and pursuit of carefully selected uni-algal continuous culture systems are proposed as the three main strategies to lead to improved economic viability [16]. Use of microalgae and perhaps other aquatic species might avoid many negative impacts on the land where alternative crop approaches are employed (erosion, eutrophication, etc) as described by *Fargione et al.* [28] and numerous others [e.g. 28, 55, 92].

Why are microalgae, and algae in general such prolific growers and consequently of interest for this application? In brief their simple structure allows for more efficient use of solar energy. While most higher freshwater plants as well as green algae and cyanobacteria make use of a more ancient form of photosynthesis (C3

---

[1]"GreenFuel Technologies Closing Down,"
http://www.greentechmedia.com/articles/read/greenfuel-technologies-closing-down-4670/
[2]"Coming Soon: $2 a Gallon Diesel From Algae?,"
http://www.greentechmedia.com/articles/read/coming-soon-2-a-gallon-diesel-from-algae/

plants) [66, 69], there is more recent genetic evidence of a more facultative nature whereby a more "modern" C4 photosynthesis and CCM (CO_2-concentrating mechanisms) approaches exist in *P.t.* and other diatoms specifically [70, 84].

Not only is the basic science of microalgae advancing; practical application too is on the rise. While still developing toward economic viability, the field of algal biofuels is promising due to it's impressive yield capacity. Even at the modest annual oil production claims from Benemann Associates for 10,000 L/Ha from pilot scale production [91], the yield is still nearly twice the annual oil yield per hectare than the next most prolific producer feedstock, palm oil (<6,000 L/Ha) [16, Table 1], without the myriad concerns of terrestrial crops (need for fresh water, food vs. fuel, etc.).

Fossil fuels are derived in part (perhaps mostly) from ancient biomass [67]; algae being a significant contributor. Consequently the aim of microalgal biofuels is simply to expedite the same process which brought us our current supply of stored ancient solar energy (fossil fuels). The target is a steady but sustainable supply of contemporary hydrocarbon fuel substitutes (biofuels).

1.4 Nomenclature

Numerous existing and thesis-specific abbreviations and terms will be employed throughout this work. A list of nomenclature including glossary terms is provided in Appendix A and should be a useful reference for those unfamiliar with the "biofuels jargon."

1.5 Thesis outline

In Chapter 2, the significance of alkenones (constitutively produced by some haptophyta) with respect to biodiesel and cold-flow performance is discussed. This is followed by Chapter 3, which details results from a practical study on Cape Cod, MA under natural solar illumination with diatoms grown on the alternative nitrogen source, urea, with and without nickel trace metal addition. Subsequent Appendices beginning on page 51 support with extended information and background to the two main chapters (2, and 3).

Chapter 2

Isochrysis, alkenones, and biodiesel cloud points

"What we're after is that chubby guy who can still run a marathon."

- Chris Reddy, Associate Scientist, WHOI; speaking in reference to the importance of lipid-productivity as a selection criteria for algal strains, not simply fast growth rates or lipid content alone.

2.1 Introduction to alkenones experiment

Interest in biofuels continues to increase with concerns over climate change and a looming energy crisis [46, 77]. Based on a resurgence of interest in microalgal-derived biofuels, it is anticipated that many large-scale bioproduction sites will be constructed in the coming decades [16, 18, 43, 44]. While this field is rapidly changing, the majority of biofuels produced at these facilities will initially be mixtures of fatty acid methyl esters (FAMEs) known as biodiesel. This substitute for fossil-fuel diesel is produced from reactions between methanol and glycerides; the latter are the major components of oil and cell membranes in microalgae as well as terrestrial plants.

Biodiesel is used to formulate a range of mixtures from B2 (2% biodiesel mixed with 98% fossil-fuel diesel) to B100 (100% biodiesel). In preparation for a future ~0.5 hectare bioproduction site in Cape Cod, Massachusetts, USA (41° 33 05"N, -70° 36 55"W), we surveyed local species capable of sustainable growth and

high production of FAMEs under the low incidence of annual light availability and cool temperatures of the region.
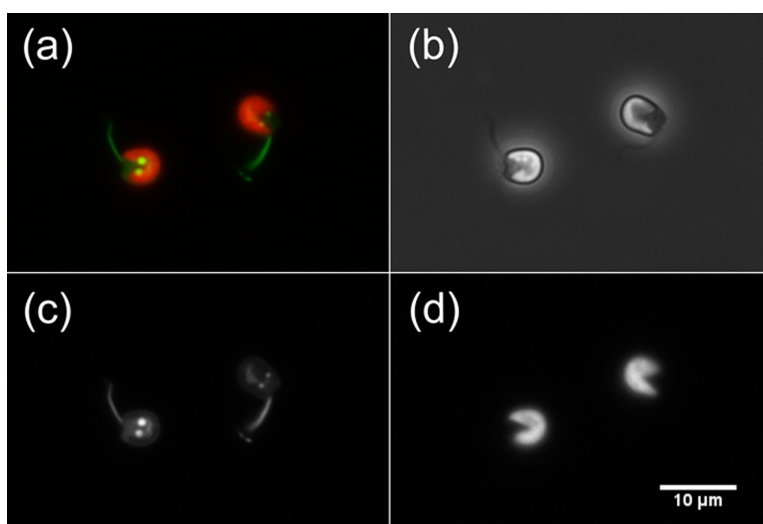
Figure 2.1: *Isochrysis* sp. (T-Iso) micrographs. (b) phase contrast image, (a) pseudo-colored merge of c and d, (c) Nile Red stained image with 46HE filter (Ex: 500/25, em: 535/30), (d) chlorophyll autofluoresence through filter set 50 (ex: BP640/30, em: BP690/50). All images acquired with Zeiss Plan-Neofluar 40x/0.75 Ph2 objective lens and Zeiss Axiocam MRm monochrome camera.

One of our targeted algae was the coastal marine prymnesiophyte *Isochrysis* sp. including strains T-Iso and C-Iso (Figure 2.1) [76, 112].We were interested in *Isochrysis* sp. as they have been cited in reviews on algal-based biofuel [16, 43], can be grown both indoors and outdoors [49], and are farmed commercially for mariculture feedstocks [5, 26, 56]. Furthermore, this effort conforms with the future fuels strategy proposed by *Inderwildi and King* [46], stressing the importance of in-depth scientific analysis of short, medium, and long-term aspects of biofuel production. Here we present results on how polyunsaturated long-chain (mainly C37–38) alkenones, part of a group of unusual compounds including alkenes and alkenoates collectively referred to as PULCAs (Figure 2.2), produced by *Isochrysis* sp. and other prymnesiophyte [20], can adversely affect biodiesel quality. Specifically, we spiked part per thousand amounts of alkenones in B20 blends prepared from soybean oil and observed the effects of the alkenones on the cloud point (CP) of the mixtures.
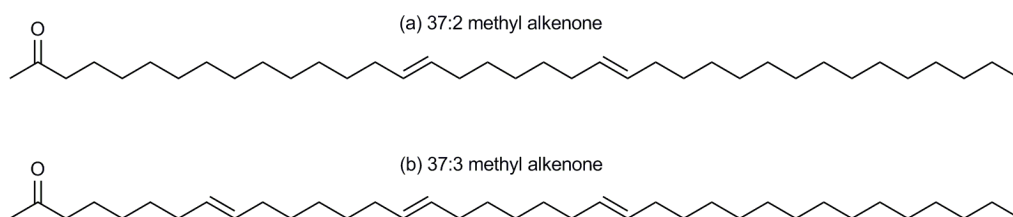
Figure 2.2: Two common alkenone structures produced by *Isochrysis* sp., exemplifying very long carbon chain and the trans-double bonds. Studies have detected methyl and ethyl alkenones with 35 to 40 carbons with two to four double bonds [86]. Nomenclature for alkenones is similar to FAMEs; # of carbons: # of double bonds.

2.2 Methods

2.2.1 Species and culture conditions

Two *Isochrysis* sp. strains "T-Iso" and "C-Iso" and the diatom, *Thalassiosira weissflogii* strain "TW" were sourced from the Milford Laboratory Microalgal Culture Collection (Milford, Connecticut). Additional information on the "T-Iso" and "C-Iso" strains has been described in detail by *Patterson et al.* [76], and *Wikfors and Patterson* [112]. We included TW in our study to highlight differences in lipid profiles of algae. Microalgae were cultured in 250-ml glass Erlenmeyer flasks under 24-hour light (approximately 31 $\mu E \cdot m^{-2} \cdot s^{-1} (PAR)$) and held on an oscillating shaker (100 rpm) at 19°C. Standard $f/2$ medium was used for cultures with silica provided for the comparison diatom (TW). Microalgae were harvested by centrifuging at 4,000 rpm and decanting the supernatant. The remaining algal pellet was freeze-dried.

2.2.2 Extraction of algal samples

Freeze-dried algal biomass (10 to 50 mg) was extracted with hexane. The resultant lipid extract was spiked with an internal standard, ethyl nonadecanoate, and transesterified under N_2 using 10% methanolic HCl in hexane (55ºC; 12 hours). We used ethyl nonadecanoate to check both the completeness of the transesterification reaction by monitoring the production of methyl nonadecanoate and using the latter for quantification purposes. The reaction products were extracted with hexane, reduced in volume, spiked with an external standard, n-heptadecane, and stored until analysis by the GC-FID.
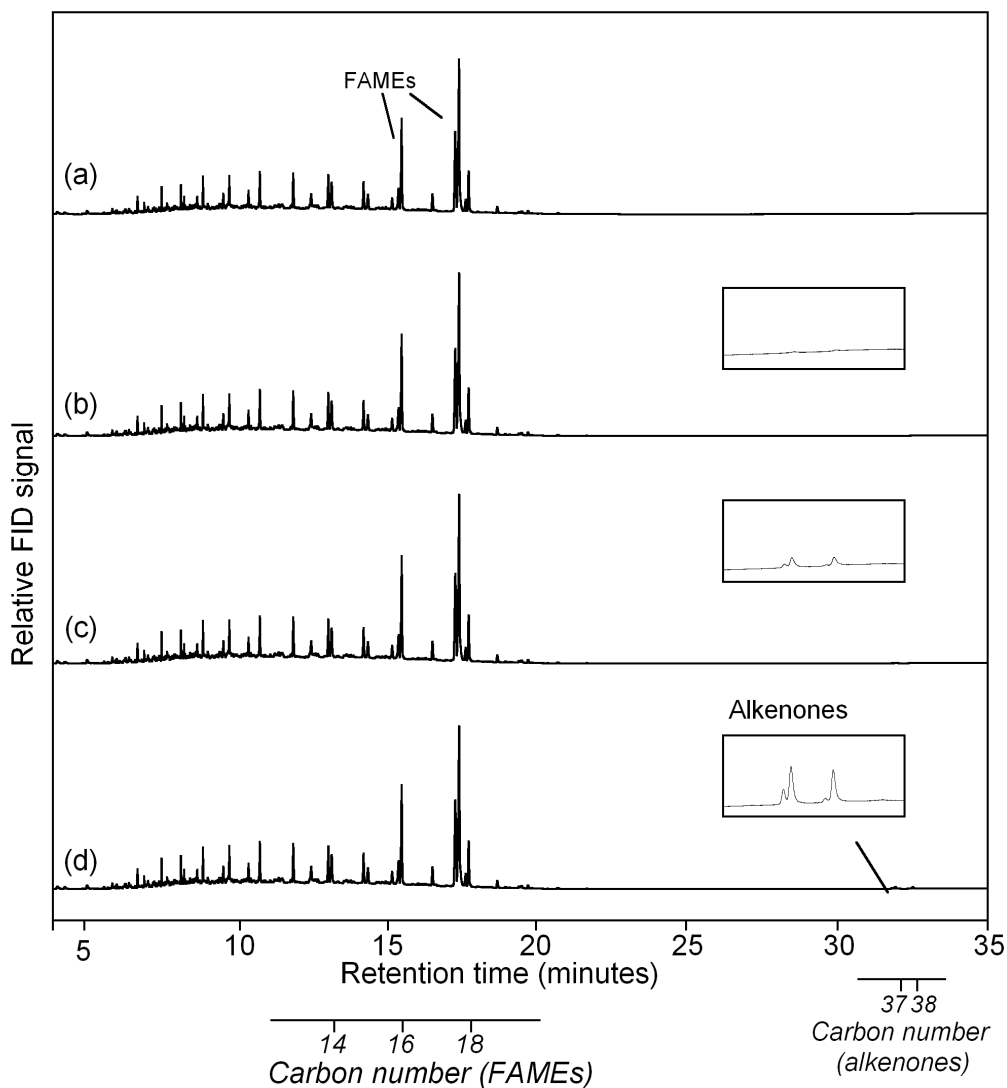
Figure 2.3: GC-FID chromatograms of B20 solutions (80% fossil diesel, 20% B100 from soybean oil) prepared for CP analysis. (a) B20, (b) B20 with alkenones (0.11 w/v), (c) B20 with alkenones (0.75 w/v), and (d) B20 with alkenones (2.25 w/v). Except for the 16 and 18 carbon FAMEs, compounds eluting in the first 20 minutes are almost all fossil diesel constituents.

2.2.3 Analysis by GC-FID

We quantified FAMEs and alkenones in the esterified samples using a Hewlett-Packard 5890 GC-FID. Compounds were separated on a glass capillary column (J&W DB-1MS, 30m, 0.25-mm i.d., 0.25-μm film thickness) with H_2 carrier gas. FAMEs were identified with standards purchased from Nu-Chek Prep (Elysian, MN) and Supelco (Bellefonte, PA). Alkenones were identified based on comparison to published elution order on gas chromatographic columns, their mass spectra, and mixtures harvested from cultures of *Isochrysis* sp. Methyl nonadecanoate recoveries were always > 90%. No ethyl nonadecanoate was observed in the samples.

2.2.4 Alkenone-spiked B20 solutions

We used a mixture of pure alkenones composed mainly of 37 and 38 carbon alkenones isolated from *Isochrysis* sp. Refer to Figure 2.3 for the relative distribution of each alkenone. We added 0, 0.11, 0.23, 0.38, 0.75, 1.13, and 2.25 mg of alkenones to 4-ml amber vials with Teflon-lined caps and then 0.8 mL of on-road fossil diesel purchased at local filling station in Falmouth, Massachusetts, USA on September 7, 2009. For the samples with higher amounts of alkenones, it was necessary to warm the vials, while capped, for 30 seconds for complete dissolution. Two hundred microliters of soybean-derived B100 (Renewable Biofuels, Port Neches, TX; passed ASTM D6751 test parameters) was then added to each vial resulting in B20 blends. The alkenone content did not affect the volume of each solution. We attempted to prepare a B20 blend with 4.5 mg of the alkenones, but the latter did not dissolve until another 1 ml of fossil diesel was added. Several microliters of each sample were removed for analysis by GC-FID. The samples were stored in darkness and analyzed for CP.

2.2.5 Cloud point analysis

The Cloud point (CP) of the fossil diesel, soybean-derived B100, and the alkenone-spiked B20 blends were analyzed with ASTM method D2500 - 09 Standard Test Method for Cloud Point of Petroleum Products. These analyses were performed by Ana Laboratories, Inc. (Newark, New Jersey).

2.3   Results and discussion
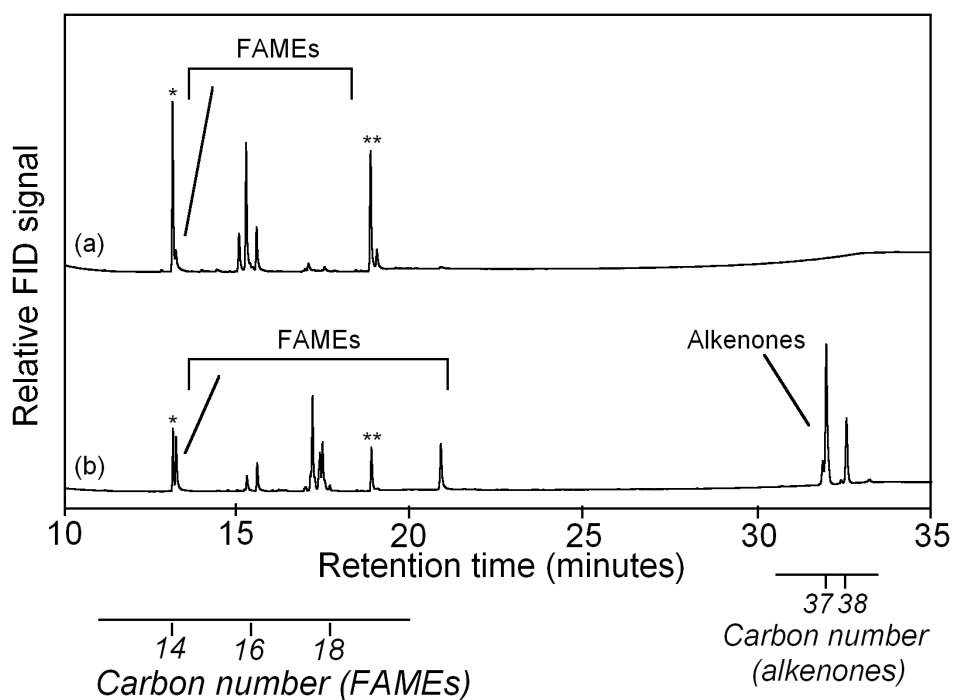
Figure 2.4: Gas chromatograms of FAMEs and alkenones extracted from marine algae. (a) marine algae *Thalassiosira weissflogii* and (b) *Isochrysis* sp. Note the absence of alkenones in the diatom (a). The peaks labeled with "*" and "**" are n-heptadecane and methyl nonadecanoate, used as standards. The FAMEs and alkenones are highlighted in the chromatograms and their respective number of carbons is labeled along the x-axis. As noted in the text, these extracts were produced from acid-catalyzed transesterification, although we found base-catalyzed transesterification yielded similar results.

During the evaluation of different algal species for biodiesel production for our region, we noticed that *Isochrysis* sp. (both strains) relative to other algal cultures was rich in alkenones with total amounts comparable to total FAMEs (Figure 2.4). This was not a surprise as it is well known that *Isochrysis* sp., *Isochrysis galbana*, and some other prymnesiophyte taxa, including *Emiliania huxleyi* and *Gephyrocapsa oceanica* produce these PULCAs [20, 29, 76, 107], with 35 to 40 carbons methyl or ethyl ketones, although 37 and 38 carbons are generally

the most dominant [86, 87]. Often these neutral lipids are more abundant than triacylglycerols, especially in the stationary-phase of growth curves [25].

Studies by *Eltgroth et al.* have shown that PULCAs reside in cytoplasmic lipid bodies for energy storage [25]. The exact biosynthetic pathways have not been elucidated, but the proportion of the more unsaturated PULCAs increases with decreasing water temperature [20, 107]. Unlike unsaturated FAMEs that have methylene-interrupted cis (Z) double bonds, the alkenones have trans (E) double bonds separated by five and occasionally three methylene groups [64, 80, 81, 86, 87] (Figure 2.2).

As *Chisti* [16] noted, not all algal oils will produce high quality biodiesel, such as those that would yield FAMEs with 4 or more double bonds, which would be highly susceptible to oxidation. However, due to their long chain lengths, double bond trans geometry, and high melting points (>55ºC) [74], we hypothesized that alkenones could be problematic, too. (Pure C36:2 alkenone has a MP of 57ºC [74], while the alkenone mixture used in this study had a MP of 65ºC.) In particular, the alkenones would likely increase CPs to unreasonably high temperatures. To test this hypothesis, we originally tried to dissolve mg quantities of alkenones into a high quality soybean-derived B100. We choose this experimental design to highlight how alkenones could affect an otherwise high-quality biodiesel. Unfortunately, we were unable to dissolve the alkenones in the soybean-derived B100 even with gentle heating. Hoping that fossil diesel would act as a solvent for alkenones, we then prepared mixtures of B20 spiked with alkenones. This approach was successful until efforts to dissolve 4.5 mg of alkenones into 1 ml of B20 failed. Preliminary solubility studies illustrate the relative insolubility and highly non-polar nature of these compounds. For instance, while the C36:2 alkenone could be dissolved in dichloromethane and benzene, it was only partially soluble in ethereal solvents, and completely insoluble in more polar solvents such as acetone and methanol.

The CP of the fossil fuel diesel and soybean B100 used to prepare the B20 mixtures were -9.4 and 2.2ºC, respectively. The B20 mixture had a CP of -6.1ºC, which increased markedly with alkenone content (Figure 2.5). In particular for B20 with 0.75 to 1.13 ppt; w/v alkenones, the CP temperature jumped from -5 to 2.2ºC, respectively. This is remarkable considering the GC-FID alkenone signal is barely perceptible even in our highest alkenone-spiked B20 sample (Figure 2.3, insets of d, 2.25 ppt; w/v), which had a CP of 20ºC. This illustrates how CP is highly sensitive to even minor amounts of non-FAME lipids, especially those with high melting points [71].

A related study by *Imahara et al.* [45] demonstrated that the addition of small amounts of higher-melting saturated esters to representative biodiesel mixtures

had a dramatic impact on CP. Importantly, irrespective of the biodiesel composition, mixtures with fixed saturated ester content had essentially identical CPs. Our alkenone-spiked biodiesel mixtures provide further evidence that CP is mainly determined by abundance of components with higher melting point temperatures. For this reason certain classes of compounds such as those with trans-double bonds have been identified that will cause a biodiesel to fail specification standards *Knothe* [53]. Others include cis-monounsaturated esters longer than C18 (melting points between approximately -8 and 9 °C), and saturated esters longer than C10 (methyl undecanoate MP = -12 °C). The long-chain length (C35 – C41), trans-alkene geometry, and resulting high melting points (>55 °C) of algal-derived long-chain alkenones make these compounds unsuitable components of biodiesel fuels.
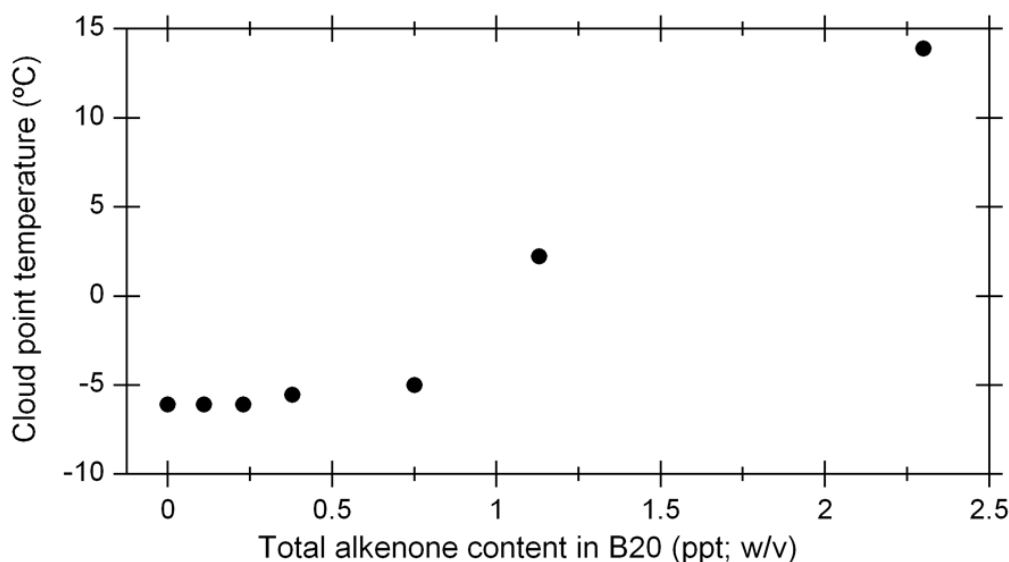
Figure 2.5: Cloud point temperature (°C) versus total alkenones content in B20 mixtures prepared from soybean-derived B100 and fossil diesel. The B20 mixtures were prepared by dissolving various amounts of alkenones into the fossil diesel and then adding the soybean B100. Error bars are smaller than symbols.

CP criteria are not strictly set by ASTM, but rather "reported," however it is likely that other regulated ASTM values would be affected, such as kinematic viscosity. In the case of CP and the related cold-filter plugging point (CFPP), ASTM D975 provides guidance for operation temperatures based on 10th percentile minimum temperatures [111]. These results are noteworthy as *Isochrysis* sp. would otherwise be a desirable producer of biodiesel amenable FAMEs. It is already

grown commercially for mariculture so any hurdles with scale-up to large scale biodiesel production would be less of a problem. We also analyzed one commercial mariculture product (T-Isochrysis Algae Paste, www.brineshrimpdirect.com) and found that it had a similar distribution of FAMEs and alkenones as Figure 2.4 (b). Moreover in a recent study of 55 microalgal species for biodiesel production, *I.* galbana proved to be average in both biomass yield and lipid productivity [35]. Average lipid content in nutrient-replete and nitrogen-deficient cultures are 25 and 29% dry weight respectively. Therefore, it is quite likely that others will be attracted to this alga's characteristics for biodiesel production, yet great care should be taken in doing so due to alkenone contamination.

Even minor feedstock components containing alkenones (levels above 1 ppt; Figure 2.5) can affect fuel quality. As shown (Figure 2.3) these compounds may elute beyond the maximum retention time and temperature gradient of a standard GC-FID analysis for biodiesel and biodiesel blends. While *Hu et al.* summarized the presence of many very-long-chain fatty acids (>C20) of several algae (including haptophyta *Emiliania huxleyi* and *I.* galbana) and cyanobacteria, the PULCAs were not considered, and indeed until now their importance may remain under-emphasized.

Synthesis of PULCAs has been documented to be restricted taxonomically within the haptophyte order Isochrysidales [19, 20]. Consequently these algae might be avoided for biodiesel unless downstream refining such as crystallization fractionation is performed [51]. However, the otherwise positive attributes of *Isochrysis* sp. noted earlier may be more ideal for generating other biofuels, such as methane from catalytic gasification of biomass that are less dependent on the lipid composition but more focused on lipid production of algae [38, 103].

2.4   Conclusions

In summary, marine microalgae have great promise for the production of biodiesel. However, some species can produce high melting-point lipids in addition to fatty acids, such as alkenones, that can detrimentally affect biodiesel quality but may be useful in other biofuel technologies.

Acknowledgments

Chapter 3

Phaeodactylum physiology and lipid quality

"This is like tuning a violin in a hail storm!"

- William (Bill) Mebane, Marine Resource Center (MRC) Systems Operator; speaking in reference to operating biological chemostats and the inherent complexities and instabilities.

3.1   Introduction to Ni/urea experiment

Diatoms are important primary producers responsible for 60% of oceanic primary productivity [101]. Furthermore, diatoms pose significant biogeochemical control on ocean primary productivity contributing 20% of global (terrestrial and marine) primary productivity [27, 30]. *Phaeodactylum tricornutum* (*P.t.*) and *Thalassiosira pseudonana* (*T.p.*) are two diatoms widely studied in culture. The genome of *P.t.* has been sequenced [13], and it is known that urea is a sutable nitrogen source for this species [83]. Urea was studied because it serves as a proxy for nitrogen sourced from waste water which is an abundant and inexpensive nutrient source for algaculture. These features justified selection of *P.t.* for this study. Physiological results and detailed lipid profiles have been prepared under treatments with only urea as a nitrogen source, versus a replete control with nitrate provided (a more conventional aqueous marine media nitrogen source). Where urea was present one treatment also had additional nickel supplemented as discussed below.
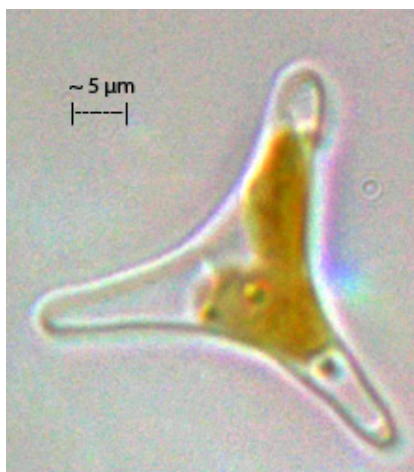
Figure 3.1: Micrograph of *P. tricornutum* (source: www.jgi.doe.gov).

Preliminary indirect evidence suggested that in the absence of sufficient nickel, cells over-produce a non-functional (apo) urease protein [82], having adverse effects on cultures growing on urea. Direct evidence, purification, and characterization of nickel-urease has subsequently been developed [105]. Broader environmental and biogeochemical ramifications of the nickel-urease continue to unfold. As proposed by *Price and Morel* [79], a colimitation effect is apparent between nickel and nitrogen with the apparent nickel-dependent urease as the likely culprit. Not surprisingly, urease was subject to numerous early scientific investigations and was the first organic molecule to be synthesized; moreover it was the first recognized nickel metalloenzyme [98]. More recently the complexity of metalloproteins and their associated chaperons was described by *Waldron and Robinson* [108]. It is evident that trace elements, micro/macro nutrients, and protein interactions behave in a dynamic and often colimiting way.

Colimitation as a concept is summarized by *Saito et al.* [90] and has been improved by recent physiology studies such as presented by *Saito and Goepfert* [89], however additional investigations such as presented here provide useful support to the modeled and theoretically purported colimitation concepts; namely with respect to nitrogen and light (independent, type I), and nickel and urea (biochemically dependent, type III) colimitations as described in *Saito et al.* [90, Table 1]. Although nickel is known to be critical for urease activity, it has other roles yet to be elucidated since even organisms lacking nickel-urease show a nickel requirement which aside from partial cobalt substitution appears to be an absolute (or type 0) requirement [100]. During photosynthesis, superoxide dismutase may also be an important nickel containing enzyme as shown in the case of some cyanobacteria [23, 24].

Urease is a nickel-dependent metalloenzyme that catalyzes the hydrolysis of urea to form ammonia and carbon dioxide.

Marchler-Bauer et al. [63] notes:

> *"Nickel-dependent ureases are found in bacteria, archaea, fungi and plants. Their primary role is to allow the use of external and*

internally-generated urea as a nitrogen source. The enzyme consists of three subunits, alpha, beta and gamma, which can exist as separate proteins or can be fused on a single protein chain. The alpha-beta-gamma heterotrimer forms multimers, mainly trimers. The large alpha subunit is the catalytic domain containing an active site with a bi-nickel center complexed by a carbamylated lysine. The beta and gamma subunits play a role in subunit association to form the higher order trimers."

P. tricornutum is one of two diatoms for which at this time genomes have been sequenced [13]. Within the genome for *T. pseudonana* (CCMP 1335), an 807 amino acid nickel urease exists (NCBI Reference Sequence: XP_002296690.1). The known urease sequence from *T. pseudonana* (XP_002296690.1) was run in BLAST against *P. tricornutum* CCAP 1055/1 (taxid:556484) producing a significant alignment with a predicted protein of 878 amino acid (accession XP_002183086). With 5% gaps in the protein alignment the positive matches were 78% yielding an e-value of 0.0. Putative conserved domain regions were detected and the conserved domain sequence "cd00375" is indeed for the nickel-dependent urease α-subunit, shown

Figure 3.2: Urease α-subunit showing the bi-nickel center complexed by a carbamylated lysine (lower right) as identified by *Benini et al.* [8].

for the aligned 567 amino acid sequence of *T.p.* in Figure 3.3 on page 20. The bi-nickel α-subunit structure is presented in Figure 3.2.

The advantage of working with an organism whose genome is sequenced may be obvious yet this is only one aspect which promoted selection of *P.t.* for this study. Ease of culturing and the ability to grow well with urea as the primary nitrogen source made *P.t.* an excellent subject for this study. Moreover, as a diatom this species represents a significant community for broader biogeochemical understanding. In general the experiment looks at "real-world" intermediate scale bioproduction with replete $f/2$ medium (*Guillard* [36], *Guillard and Ryther* [37]) versus a nitrate-free $f/2$ amended with urea to serve as a proxy for the

uric acid sourced from urine in waste water. An additional experimental treatment included both urea and nickel. Sampling was performed daily for relative fluorescence (a proxy for biomass and the basis of growth-curve data), and approximately every other day for approximately 2 weeks looking at the following parameters: (1) relative fluorescence units (RFU), (2) biomass (dry weight), (3) lipids and proteins, (4) nutrients and nickel, (5) flow cytometry.

A key determinant in evaluating microalgal strains for biofuels potential, particularly with respect to biodiesel is the lipid distribution. Information regarding hydrocarbon chain length, prevalence of double bonds, and bond type are crucial aspects in sorting microalgae candidates as noted in Chapter 2. Consequently, detailed GC-FID analysis has been performed on the transesterified oil products from algae extractions over the range of growth stages and treatments from this experiment (Sections 3.3.3 and 3.3.4).


```
CD Length: 567  Bit Score: 839.13  E-value: < 1.0e-180
                    10        20        30        40        50        60        70        80
                ....*....|....*....|....*....|....*....|....*....|....*....|....*....|....*....|
gi_224014054 226 LTRSAYSDAYGPTTGDRVRLGDTSLIARIQADHTHYGDECKFGGGKSLREGMGQMTSVSASLALDCVITNAMIIDAkLGI 305
Cdd|cd00375    2 ISREAYADMYGPTTGDKVRLGDTDLWIEVEKDYTTYGDEVKFGGGKVLRDGMGQSSGYTREDVLDLVITNALIIDY-TGI  80

                    90       100       110       120       130       140       150       160
                ....*....|....*....|....*....|....*....|....*....|....*....|....*....|....*....|
gi_224014054 306 IKADIGIKGNKIHNIGKAGNPDTMNGVTltpgKEMIVGATIDVIAGEKMIVTAGGVDTHIHFICPQQCDEAIASGVTTMF 385
Cdd|cd00375   81 YKADIGIKDGRIVAIGKAGNPDIMDGVT----PNMIVGPSTEVIAGEGKIVTAGGIDTHVHFICPQQIEEALASGITTMI 156

                   170       180       190       200       210       220       230       240
                ....*....|....*....|....*....|....*....|....*....|....*....|....*....|....*....|
gi_224014054 386 GGGTGPSAGTSATTCTPGPGHVEMMLRATDDLPLNFGFSGKGNTSDPNtSIIDVLRSGASGFKLHEDWGTTPSAIDACLT 465
Cdd|cd00375  157 GGGTGPAAGTKATTCTPGPWNIKRMLQAADGLPVNIGFLGKGNGSSPD-ALAEQIEAGACGLKLHEDWGATPAAIDTCLS 235

                   250       260       270       280       290       300       310       320
                ....*....|....*....|....*....|....*....|....*....|....*....|....*....|....*....|
gi_224014054 466 FADEHDVQVTIHTDTLNESGYVDDTLRAVKGRTIHAYHTEGAGGGHAPDIMKIVRESNVLPSSTNPTRPFTRNTIDEHLD 545
Cdd|cd00375  236 VADEYDVQVAIHTDTLNESGFVEDTIAAIKGRTIHTYHTEGAGGGHAPDIIKVAGHPNVLPSSTNPTRPFTVNTLDEHLD 315

                   330       340       350       360       370       380       390       400
                ....*....|....*....|....*....|....*....|....*....|....*....|....*....|....*....|
gi_224014054 546 MLMVCHHLDPSIPEDVAFAESRIRPETIAAEDILHDLGALSMISSDSQAMGRVGEVITRTWQTADKMKQQLGPLEEDAAN 625
Cdd|cd00375  316 MLMVCHHLDPNIPEDVAFAESRIRAETIAAEDVLHDLGAISIMSSDSQAMGRVGEVILRTWQTAHKMKAQRGPLPEDSGD 395

                   410       420       430       440       450       460       470       480
                ....*....|....*....|....*....|....*....|....*....|....*....|....*....|....*....|
gi_224014054 626 ShpdgldDNERILRYVAKYTINPAIAHGMSHLIGSIESGKLADLVLWKPSTFGAKPEMIIKGGAIAWAQMGDPNASIPTP 705
Cdd|cd00375  396 A------DNFRVKRYIAKYTINPAIAHGISHEVGSVEVGKLADLVLWEPAFFGVKPEMVLKGGFIAYAQMGDPNASIPTP 469

                   490       500       510       520       530       540       550       560
                ....*....|....*....|....*....|....*....|....*....|....*....|....*....|....*....|
gi_224014054 706 QPVYMRPMFGArprVAGDGGGTSIAFVSNMAATDGIGERLGLGKEVASVVGTRHVSKADMVRNDATPDIRIDPETFEVVA 785
Cdd|cd00375  470 QPVMMRPMFGA---HGKAPAATSVTFVSQASLDAGIAEELGLRRRVVAVKNCRGVGKKDMKLNSATPDIEVDPETYEVRV 546
```

Figure 3.3: Conserved domain (bottom line) for nickel urease α-subunit against *P.t.* (top line), amino acid matches are highlighted throughout.

3.2   Methods

3.2.1   Fluorescence (RFU)

Fluorescence data was collected from a Turner Designs TD-700 bench-top fluorometer with filters configured to measure chlorophyll a (PMT 185-870 nm, ex: 340-500 nm, em: >655 nm). Daily calibration was performed with a solid standard turned to the "high" orientation. Dilution was necessary to avoid signal saturation in dense cultures of late exponential phase. Samples were measured after dilution in 1 cm path-length glass test-tubes with equal parts sample and filtered seawater of the same source as used in culture media preparation (Vineyard Sound seawater, Cape Cod, MA). All recorded data is relative to the solid standard and serves as a proxy for cell concentration.

3.2.2   Biomass (dry weight)

Samples for dry weight were collected by gentle (<35 kPa) vacuum filtration of 250 mL of sample onto preweighed and combusted Whatman GF/F filter paper. Filters were dried overnight at 60ºC and subsequently re-weighed and normalized to filtered culture volume for dry wight biomass in units mg/L. These samples were archived for future TOC and biogenic silica analysis. Biomass productivity values are calculated from the net increase/decrease in biomass divided by the elapsed time relative to any sampling time-point.

3.2.3   Lipid and protein pellets

Biomass for subsequent lipid extraction was collected by centrifugation (Beckman J2-21M, rotor #14) at 9,000 rpm (12,600 x g) for 25 minutes at 10ºC. Pellets from two 250 mL volumes were combined and centrifuged at 13,000 rpm in an eppendorf MiniSpin micro-centrifuge. Supernatant was decanted and the remaining pellet was freeze dried and stored at 4ºC until extraction detailed in Section 3.3.3 on page 32. Proteomic pellets were prepared in a nearly identical way to those for lipids with the only alteration being that biomass pellets were immediately stored at -80ºC after pelletization.

3.2.4   Nutrients and nickel

Nutrient samples were collected by syringe filtering (0.2-μm) ~45 mL of culture into 60 mL acid-washed vials. All samples were frozen until analysis which was

done at the Woods Hole Oceanographic Institution (WHOI) nutrient processing facility. Nickel samples were prepared by the same methods as for nutrients, however only the +urea, +nickel treatment was tracked throughout the entire time-course. Replete and +urea, -nickel treatments were sampled for nickel only at start (t_0) and end (t_f) of the experiment.

3.2.5 Flow cytometry

Small 1.8 mL volumes of sample were mixed on ice with 0.2 mL chilled formalin (10% by volume Formaldehyde [~36%] buffered in $f/2$ medium). Cryo-vials with the fixed samples were stored in liquid nitrogen archive for future flow cytometry analysis.

3.2.6 Algaculture

Detailed algaculture culture medium methods are outlined in Appendix C.4. Briefly, a common $f/2$ media developed by *Guillard* [36], *Guillard and Ryther* [37] was used as has been typical of numerous previous physiology studies. The only exception to medium preparation was in sterilization methods; here either microwave or chlorine bleach with subsequent sodium thiosulfate addition was employed (details described in Appendix C.4.2).

Maintenance cultures of *Phaeodactylum tricornutum* (strain number CCMP632) were kept in a growth chamber at 23ºC with constant light of ~160 $\mu E \cdot m^{-2} \cdot s^{-1}(PAR)$. Maintenance cultures were 1 L, followed by primary acclimation cultures also at 1 L to allow for adjustment to treatment conditions. Subsequent scale-up to 8 L and finally 80 L was done during exponential growth with approximately 5-10% inoculation volumes to establish approximately equal relative fluorescence across treatments. Cultures subsequent from and including the 8 L scale were grown in a greenhouse kept between 12 and 25ºC (time and weather dependent) under natural diurnal illumination.

Conditions for all acclimation cultures (1 L and 8 L scale) were the replete $f/2$ control in addition to two experimental treatments where nitrate was replaced by urea at half the molar concentration (as two nitrogen atoms exist per urea molecule versus the single nitrogen in a nitrate molecule). In one of the urea treatments nickel was also provided at a total added concentration of 100 nM. In the final 80 L experiment these media conditions were sustained with the single exception being that double the phosphate was inadvertently added in the replete media.

Throughout maintenance and 1-L scale acclimation, cultures were bubbled continuously with atmospheric air filtered by 0.2-μm filters. For practical reasons the air supply to 8-L acclimation and 80-L experimental cultures was passed through a column approximately 10 cm long and 2 cm in diameter, lightly packed with glass wool to remove only larger particulates from the centralized greenhouse air supply.

The greenhouse was positioned on the WHOI Quissett Campus, Cape Cod, MA (41° 33 05"N, -70° 36 55"W, 7 m elevation). Greenhouse siting allowed significant solar exposure (i.e. minimal shading) even in winter months and the building and culture array were oriented with the long-axis aligned to an east-west direction (Figure 3.4) allowing for minimal self-shading.

Figure 3.4: Greenhouse site and surroundings - Google Earth image with building at center outlined by box east of the baseball diamond's left-field (north oriented to top).

3.2.7 Total lipid extract

Pellets of approximately 50 mg (dry weight) were accurately weighed then transferred to a Soxhlet thimble which was placed into a combusted glass vial and extracted in 20 mL of dichloromethane/methanol (2:1). Extractions were incubated at 70ºC for 1 hour before decanting solvent. Three sequential incubated solvent extractions per pellet were combined to obtain a figure for total lipid extract (TLE). The TLE was reduced in volume by rotovap and blown down to dryness under gentle UHP nitrogen gas allowing for an accurate extraction mass. Using TLE, the lipid content was determined and expressed as a percent of original biomass dry weight. TLE was resuspended for storage further analysis in

hexane containing 0.25% butylated hydroxytoluene (BHT) (to prevent/minimize sample oxidation).

3.2.8 Transmethylation

Transmethylation (transesterification) was performed on an aliquot of TLE to convert TAGs to the component fatty acids. Acid catalyzed transmethylation of lipids was conducted in combusted glassware. Methanoic HCL was prepared by gradual (dropwise) addition of 5 mL of acetyl chloride in 50 mL of cool-dry methanol [17]. For this study, 0.2 mL of TLE was taken from each sample, brought up to 1 mL in hexane then combined with 2 mL of methanolic HCL and 0.5 mL of ethyl nonadecanoate (C19 FAEE) internal standard (141 micrograms). Vials were then purged for 1 minute with UHP nitrogen, capped quickly, and the cap-glass interface wrapped with Teflon tape. Samples were incubated at 70ºC for 4-6 hours to ensure complete methylation.

Following incubation vials were cooled to room temperature and the solution was washed as described here: (1) add 10 mL deionized water and (2) 10 mL hexane, then (3) gently invert 6 times prior to centrifugation (1500 RPM, 5 minutes) followed by (4) decanting all hexane and (5) repeating all from step 2 twice more.

The washed product (combined hexane decants) was reduced by rotovap and then dried under gentle UHP nitrogen gas to allow for a measure of total conversion from TLE to methylated oil product (MOP). After MOP mass was recorded, all samples were resuspended in 1 mL of hexane containing 0.25% BHT as described in section 3.2.7.

The internal process standard ethyl nonadecanoate (ethyl-C19 or simply C19) was added to track methylation efficacy and wash recovery; if the transesterification reaction does not go to completion the ethyl peak (C19-FAEE) will appear in subsequent GC-FID analysis independent from the methyl peak (C19-FAME). As the internal standard addition of C19 is known, it serves as a quantification standard for sample FAMEs with known internal response factors. Previous work has shown high conversion efficacy (ethyl to methyl).

3.2.9 GC-FID quantification

A target of approximately 50-100 $ng/\mu L$ on column was achieved by diluting the MOP in hexane. Since most samples were approximately 0.23-1.2 mg/mL, a common $1/10^{th}$ dilution provided the practical 23-112 $ng/\mu L$ MOP on column.

Included in the dilution at final volume of 1000 uL was an external standard spike of n-heptadecane (nC17) for quality control purposes. The external standard is not necessary, nor common but was used as an added quality control measure and to determine recoveries of the internal standard. Quantifying the methyl nonadecanoate required adjustment for the lost carbon in conversion from FAEE to FAME (Details, see Appendix C.3.2). In brief, C19 FAME was simultaneously used to determine recovery (based on nC17) and to calculate compound specific amounts based on IRFs which are generally 1 for hydrocarbons. Nonadecanoate (C19) and n-heptadecane (nC17) are valid standards because they have odd-numbered carbon lengths which are not expected in these natural samples on account of the biosynthesis pathway for fatty acids which results in even-numbered carbon chain lengths.

FAMEs in the esterified samples were quantified with an Agilent 5890 GC-FID. Compounds were separated on a glass capillary column (J&W DB-1MS, 30m, 0.25-mm i.d., 0.25-μm film thickness) with H_2 carrier gas. The injection volumes for GC runs were 2 microliters, and the temperature program began with a 5 minute hold at 40ºC, followed by a 30ºC/min ramp to 120ºC, proceeding immediately then at 8ºC/min until reaching the final 320ºC which was held for 5 minutes.

Results of GC-FID analysis were processed with standard internal response factor methodology, taking the resulting specific quantified compounds and normalizing to biomass. Further details on the GC-FID methodology are presented in Appendix C.3.

3.2.10 Environmental monitoring

Representative temperature logs were prepared from a simple data-logging multimeter (Fluke 189) equipped with a type K thermocouple exposed to air or submerged in an abiotic 80 L culture tube for approximately 48 hours. Global shortwave solar radiation was sourced from Dr. Richard Payne (WHOI) as measured in 1-minute intervals by an Model PSP Pyranometer (Eppley Labs, Newport, Rhode Island) over the range 0.285 to 2.8 μm. The 1-minute averages were subsequently averaged into 15-minute data for the purposes of this study. Integration of total daily solar energy were taken over the 15-minute averaged data set.

3.3 Results and discussion

First evidence of variation between treatments was observed in the acclimation cultures where the urea treatment without added nickel lagged slightly behind the other cultures as determined by RFU (data not shown). The 8 L acclimation cultures were grown in a greenhouse where environmental parameters varied within controlled temperature set-points. Light and temperature from a representative ~48 hour period can be seen in Figure 3.5.
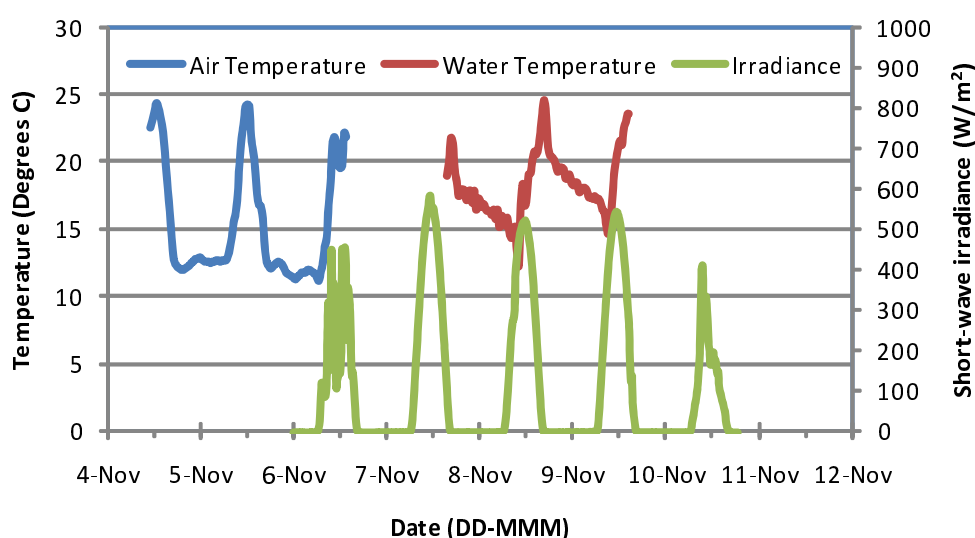
Figure 3.5: Representative temperature and light conditions each recorded over approximately 48 or more hours during November in an east-west long-axis aligned greenhouse.

During algaculture, rigorous aseptic technique was not practical, however all reasonable efforts were made to minimize contamination – keeping relatively high cell densities and typical inoculation volumes ~10% helped ensure contamination could not easily compete with the desired *P.t.* biomass. Cultures were monitored by microscopy and no notable contamination was seen except for minor fungal contamination by the late exponential phase (day 6) at 80 L scale. Due to the high fluorescence and optical cell densities in addition to the practical approach of this work, the minor fungal contamination observed late in this study were not considered a compromise to the results. It is valuable information to know that at least through several generations up to 80 L culture volumes very little contamination was observed.

Of the samples collected, not all were processed for this presentation and consequently the following results are limited to (1) growth data from RFU measurements, (2) biomass time-course (dry weights), (3) nutrient data (NH_4, NO_2+NO_3, Si, PO_4), and (4) TLE and lipid (FAME) distribution.

3.3.1 Growth curves and biomass productivity
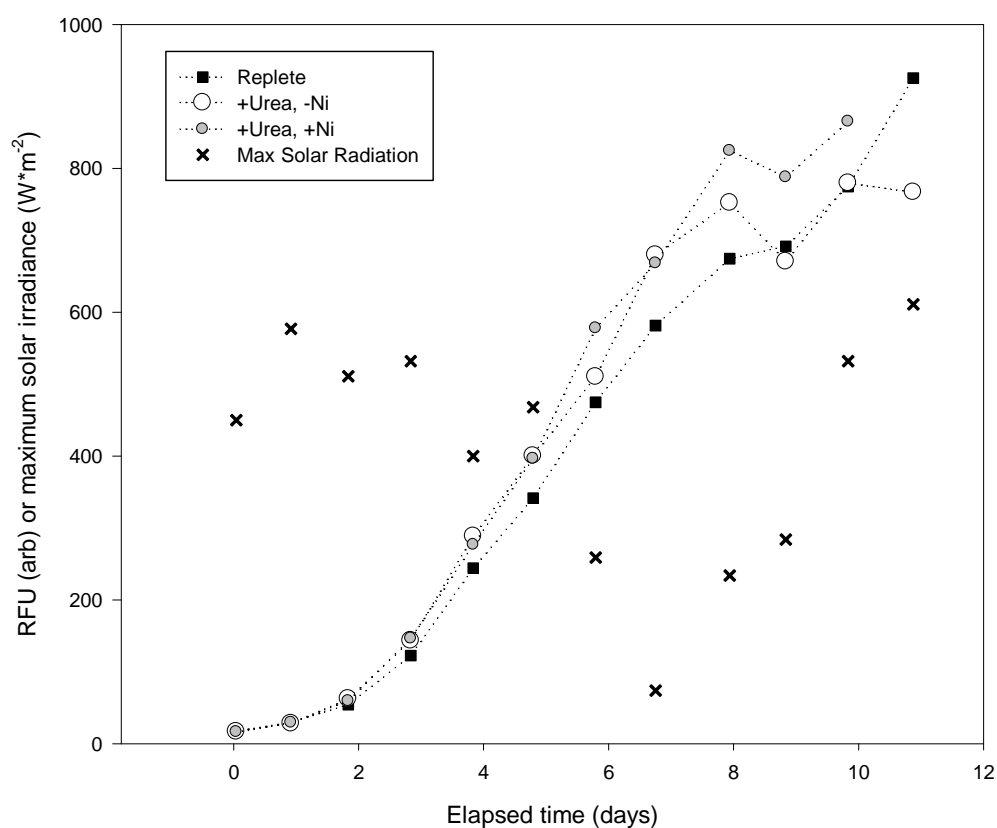
Figure 3.6: Growth curves and maximum solar radiation for all treatments at 80 L scale.

Growth curves (RFU vs. time) show typical exponential and stationary phases and are plotted along with the maximum solar radiation in Figure 3.6. Biomass alone including a late harvest time-point (day 41) is presented in Figure 3.7. The late harvest was impromptu, however it is speculated that the divergence noted at day 41 would have been present (perhaps to an even greater extent) much earlier than day 41.
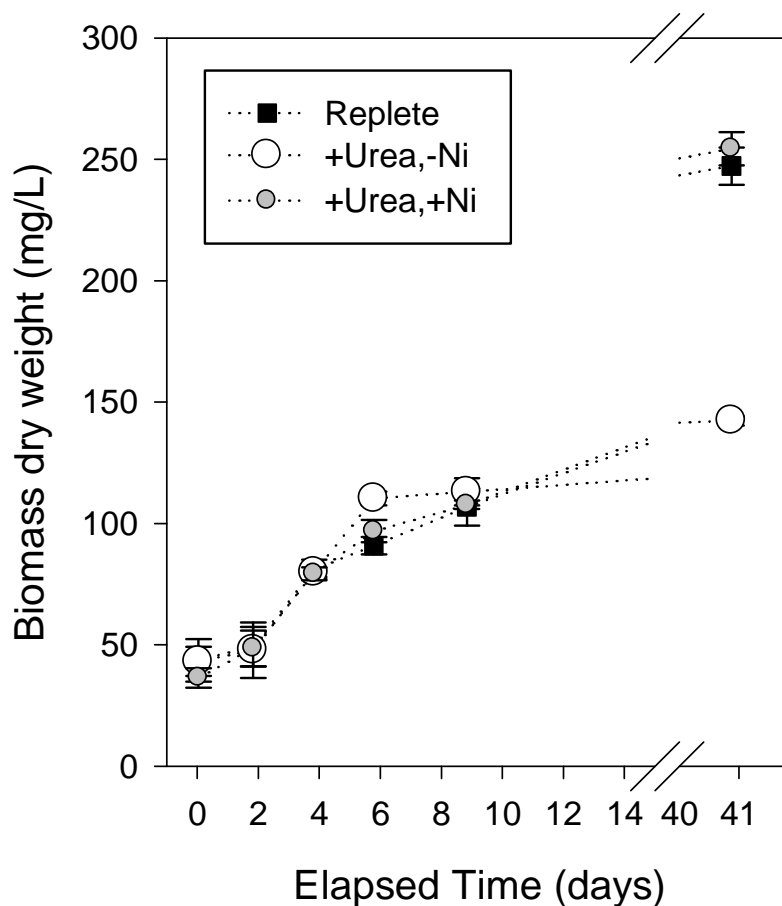
Figure 3.7: Biomass dry-weight vs time.

Biomass was beginning to proliferate when an uncertain blend of simultaneous light and nutrient limitations set in. For the purposes of this discussion the notable time-points discussed will be early exponential (day 2), mid-exponential (day 4), late exponential (day 6) and "stationary" (day 9). Light limitation may have induced a premature appearance of entry into "stationary" phase, hence the quotes used here when referring to "stationary" phase.

At day 41 significant biomass accumulation persisted in both the replete and +urea, +nickel treatments; conversely, the +urea, -nickel treatment underperformed (Figure 3.7). This is strong evidence that nickel is a beneficial nutrient through or during late growth phases when grown on urea.
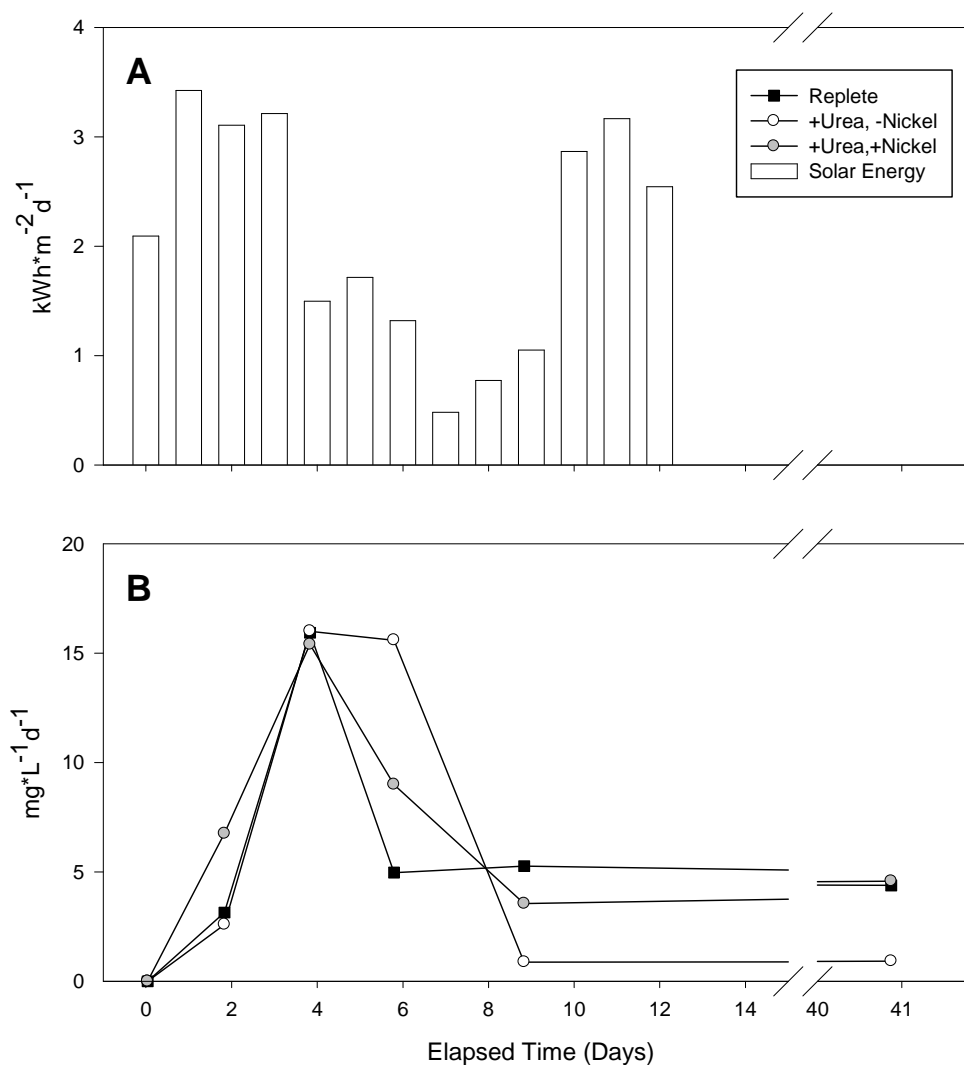
Figure 3.8: (A) Total solar energy inputs and (B) biomass productivity over 41 days.

Biomass productivity for all treatments attained a local maximum between days 2 and 4 (true exponential growth phase) (Figure 3.8 (B)). The calculated biomass productivity at this resolution is very enlightening because it can be compared directly with the nutrient, light, fluorescence, and other parameters of this study. Furthermore, it is encouraging to note that the productivity values measured here (>0.015g/L/day) are within an order of magnitude of laboratory results for the same species presented by *Rodolfi et al.* [85] (0.24 g/L/day). This comparison of results is further compelling considering the lab-cultured results were

highly catered to, having been grown with replete $f/2$ medium in 250-mL Erlenmeyer flasks (100 mL of culture) maintained in an orbital incubator flushed with air/CO_2 (95/5, v/v) at a temperature of 25°C, under continuous illumination (100 $\mu mol\, PAR\, Photons \cdot m^{-2} \cdot s^{-1}$). In comparison we used the same f-medium (*Guillard and Ryther* [37]) but under natural light conditions, minor atmospheric air bubbling lacking CO_2 enrichment (for mixing and provision of CO_2) and significantly cooler temperatures than the *Rodolfi et al.* study.

The large 80-L culture volume and significant culture density virtually assures substantially reduced solar exposure in comparison with any lab study. *Chisti* [16] notes and compares the reported half-saturation constant of light for *Phaeodactylum tricornutum* which is 185 $\mu mol\, PAR\, Photons \cdot m^{-2} \cdot s^{-1}$ [62], or about 20 $W \cdot m^{-2}$. Although solar irradiance can be well above this, it would soon reach an inhibitory region whereupon stress would prevail.

Natural lighting will follow a roughly gaussian shape, increasing from dawn to a mid-day peak then fading into dusk; consequently for a more accurate comparison the reported photon irradiance should be converted to energy irradiance and then integrated over the comparison duration (24h). Daylight fluorescent tubes are meant to simulate natural sunlight (color temperature of 5500K in accordance with our sun). As cultures are typically illuminated directly, the PAR fluence and PAR irradiance are synonymous and the relation of equation 3.1 may be applied [104, Chapter 9, topic 9.1].

$$2000\,\mu mole\, PAR\, photons \cdot s^{-1} = 400\,W \implies \frac{5\,\mu mole\, PAR\, photons}{W \cdot s} \qquad (3.1)$$

Hence, lab lighting is approximately $20W \cdot m^{-2}$ (100/5).[1] Taking continuous lighting, (24 h/day), the PAR irradiance on a per-meter basis yields daily energy of 0.48 $kWh \cdot m^{-2} \cdot day^{-1}$(0.02kW/m^2 * 24h/d). *Taiz and Zeiger* note that when light is completely diffuse, irradiance is only 0.25 times the fluence rate which is likely within the naturally-lit greenhouse environment. Still, taking the best case (direct sunlight), the solar energy inputs would be on the order of 2000 $\mu mol\, PAR\, photons$ or 400 W (roughly 40% of the 1000 W total solar irradiance typically measured in clear and sunny conditions); thus the daily solar energy for this experiment on a per-meter basis ranged from 0.19-1.3 $kWh \cdot m^{-2} \cdot day^{-1}$ (40% of the minimum and maximum values in Figure 3.8, A). On the

---

[1]This is an acceptable approximation for conditions as defined, however this is a great simplification from the actual electromagnetic radiation physics which require Plank's Law integrating the spectral radiant emittance over the desired wavelength range.

sunniest day then the PAR energy would be at most 2.85 times laboratory conditions, however on cloudy days it is less than half the laboratory-case total daily irradiance. Because the solar energy was measured outside the greenhouse, and days were not always clear it is certain that cultures were exposed to less input PAR than the lab conditions of *Rodolfi et al.* [85].

3.3.2 Nutrient data
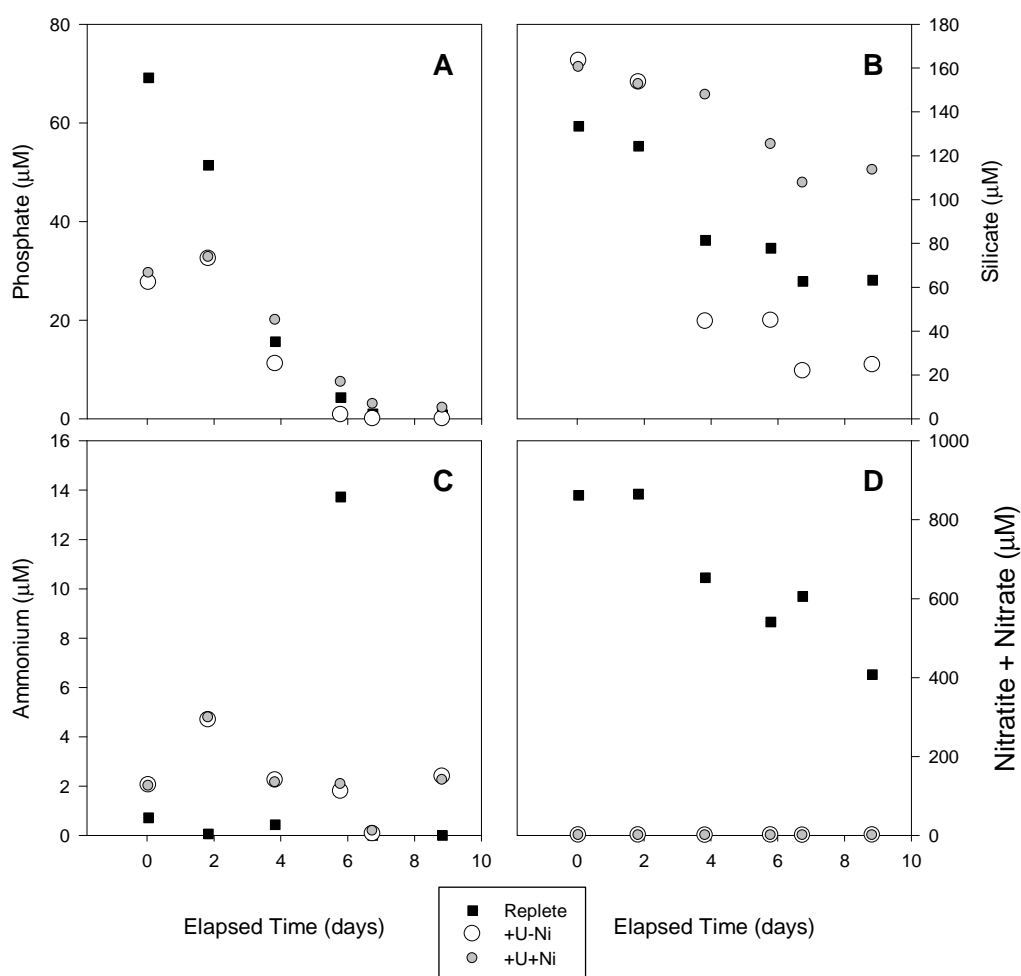
Figure 3.9: Nutrients: (A) phosphate, (B) silicate, (C) ammonium, (D) nitrate+nitrite.

N:P ratios were initially ~25 for both urea treatments and ~12 for the replete control. By day 9 the dissolved N:P was over 500 in the replete media. Nutrient

draw-down is especially evident in phosphate and silica (Figure 3.9, A and B). Although phosphate was inadvertently added in excess to the replete culture, it tracked with the experimental treatments by day 4. Silica draw-down in the urea treatment in absence of nickel exceeds the moderate draw-down in the presence of nickel and intermediate results with replete media (where no additional nickel was provided).

With respect to the silica data, some insight may be provided in consideration of oceanographic biogeochemical literature such as presented by *Firme et al.* [31] and *Dupont et al.* [23] regarding silica and nickel biogeochemistry respectively. For example *Firme et al.* postulate that silica is only depleted after iron – perhaps similarly in the no-added nickel treatment silica is more quickly depleted due to nickel limitation. This is particularly compelling as *Dupont et al.* notes the importance of nickel in SOD, independent of the nitrogen source. A cursory BLAST with the putative NiSOD from *Prochlorococcus marinus* str. MIT 9301 (YP_001091703) against *P.t.* yields a dozen significant alignments and there are several conserved domain fragments from the NiSOD. Consequently, urea only (no added nickel) culture may have been unable to resolve oxidative stress in addition to having limited ability to metabolize urea.

No significant quantities or trends were observed in ammonium (Figure 3.9, C), indicating that this intermediary in urea metabolism was quickly depleted. No measurable levels of combined nitrate and nitrite were detected in the urea treatments, and in the replete culture medium, this analyte was gradually drawn down to about half the initial concentration (Figure 3.9, C) which in light of the high final N:P ratio shows phosphate became more limiting than nitrogen in this culture.

It is apparent from the nutrient data and biomass/RFU in conjunction with light data that these cultures may have undergone simultaneous limitations of light and macro-nutrients. Initially it is thought that light became limiting especially after observing cell densities by day 4 which were sufficient to cause significant internal shading.

3.3.3 Total lipid extract (TLE)

Total lipid extract is an important figure for comparison because it closely reflects the potential for raw oil production normalized to biomass which can help establish bounds on biodiesel production estimates. Resulting TLE for the treatments and time points of this study are presented in Figure 3.10.
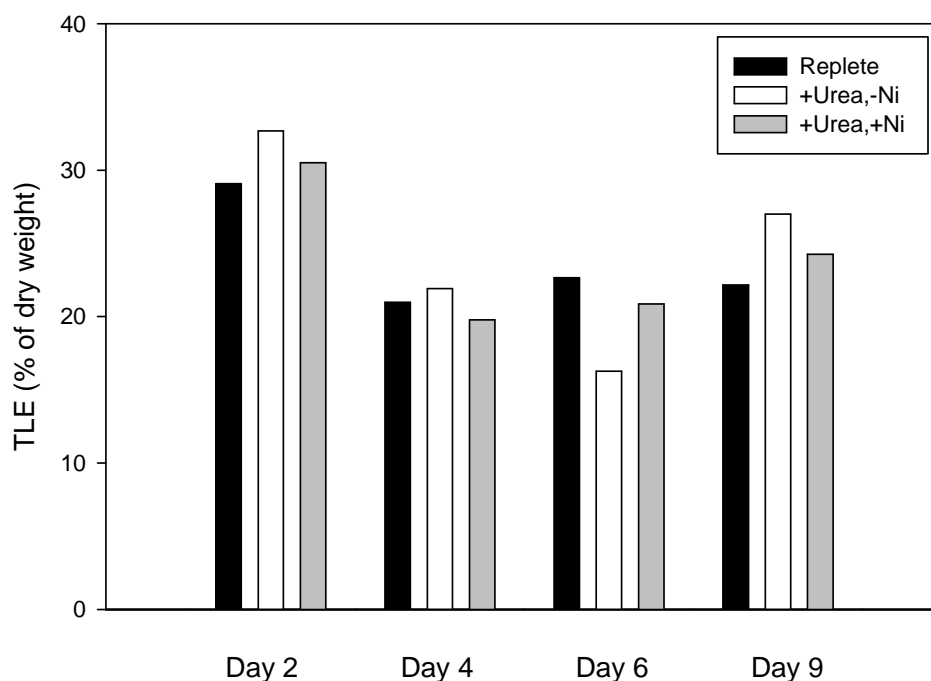
Figure 3.10: TLE as percent of dry weight biomass.

The approximate range of TLE for this study is 15-30% with an overall average of all time-points and treatments being 24% matching well with the published values of 21 and 23 % for replete and N-deficient cultures respectively in a review including six reference papers specific to *P.t.* [35]. The significant aspect of TLE presented here is the difference between early exponential growth phase (day 2) and all subsequent time-points. It seems at first counter-intuitive for the TLE to drop with declining nutrients (particularly nitrogen in the case of the replete culture), however this may be an indication that significant (albeit temporary) light limitation existed, causing increased catabolism as a measure to counter-act the lower abundance of solar energy noted in Figure 3.8, A.

While TLE is a useful indicator, it warrants comment, that this is a "bulk" indicator. Just as chlorophyll has been a simple indicator with more advanced pigment analysis often being more revealing; here too TLE is a simple practical tool. Detailed lipid profiling can provide more insight than TLE alone; such profiling is summarized in the the following section.

3.3.4 FAME distribution
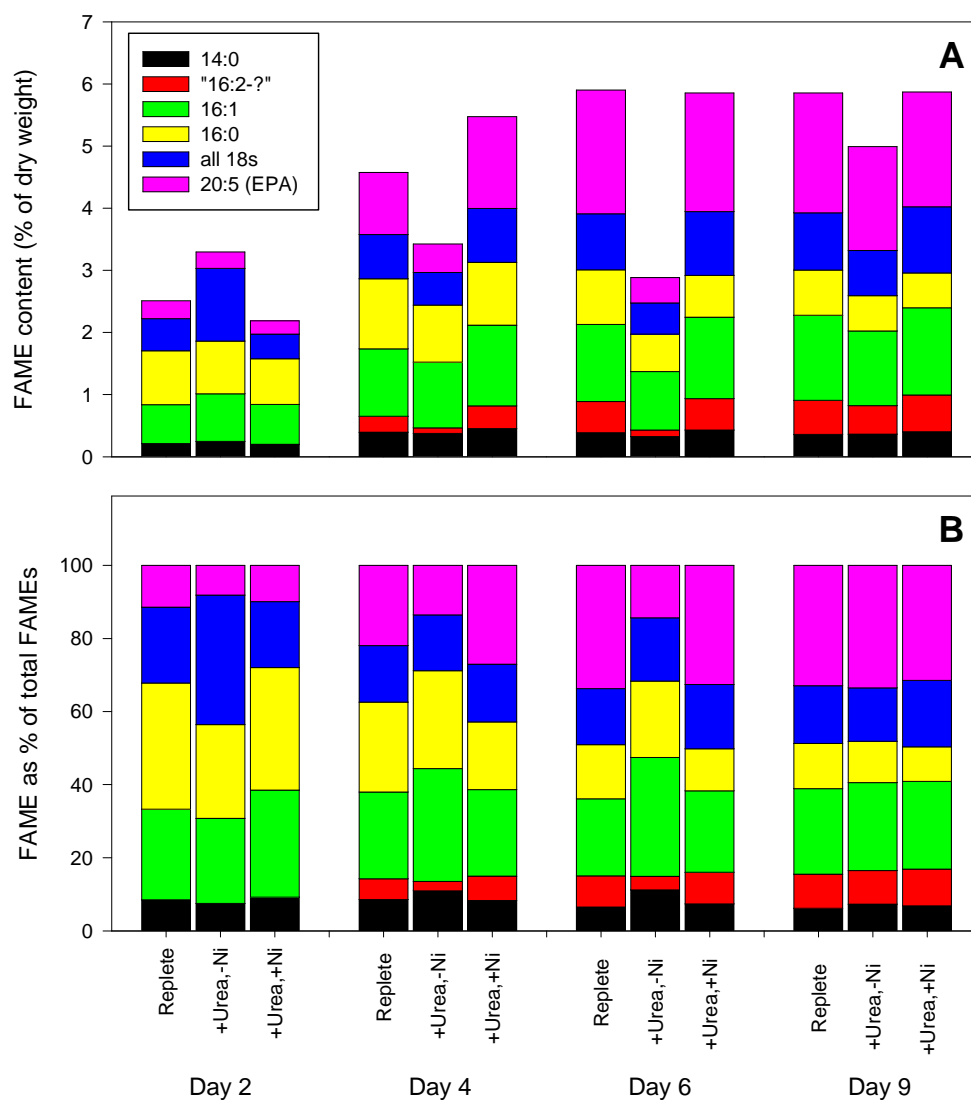
Figure 3.11: FAME distribution; as percent of (A) dry weight biomass and (B) total FAMEs (i.e., FAME as % of total FAMEs).

In addition to TLE (a quantity measure), the specific FAME distribution reveals the "quality" potential of a given microalga strain, treatment, or harvest time. As a quality control measure, transesterified canola oil was compared with experimental extractions and documented FAMEs content – encouragingly these mea-

surements were identical to literature values (details in Appendix D.2). It should be noted also in quality control that ethyl nonadecanoate was **not** detected in any GC-FID results indicating thorough transesterification.

All but one compound was verified with standards purchased from Nu-Chek Prep (Elysian, MN) and Supelco (Bellefonte, PA). The unverified peak is most likely 16:2 (or 16:3) FAME, but as this was not explicitly confirmed it will be referred to here as "16:2-?" to signify the uncertainty. Future work by GC-MS, or a simple hydrogenation experiment will confirm the speciation of this compound.

Lipid extracts were processed for FAME content on days 2, 4, 6, and 9 with recoveries all >89%. Because internal standards were used for quantification, even with recoveries below 100% the results are valid and reliable. Results can be summarized concisely as the biomass dry-weight normalized quantities of main component FAMEs. Component FAME ratios and total FAMEs are simultaneously depicted for all treatments and time-points in Figure 3.11.

Compared with TLE it can be noted that a more significant FAME trend exists among treatments (in addition to growth phase). While TLE generally declined after day 2, the FAME content normalized to biomass actually raises (increased ratio of storage- versus membrane-lipids). Furthermore, the FAME content of the urea treatment lacking nickel (+urea,-nickel) was highest on day 2, but subsequently lowest for all other time-points. FAME content in the replete and nickel amended urea treatment compared well with each other throughout the experiment.

A contributor to the elevated FAMEs following day 2 is the putative 16:2 FAME (Figure 3.11(A),"16:2-?") and to an even larger extent EPA which in the replete and nickel added treatments intensified to >30% of the FAMEs (compared to a preliminary value, 10%). Other such changes in the FAMEs distribution are summarized in Figure 3.11(B).

3.3.5 Literature intercomparison and further discussion

A recent and related study on TAG accumulation and profiling of *P.t.* during starvation (*Yu et al.* [117]) notes that chemotypes of the TAGs produced were generally similar regardless of the starvation condition. FAME results presented here appear to corroborate the *Yu et al.* study with respect to similarity of chemotypes.

For days 4 and 6, the dominant compound was eicosapentaenoic acid (EPA, a 20:5 compound) except in the urea treatment without nickel added. This compound although holding potential for use in nutraceuticals [116], is less desirable

for biodiesel by the prevailing transesterification production methods. As discussed in in Chapter 2, alternative conversion strategies exist such as hydrothermal gasification[38, 103].

As originally proposed by *Yongmanitchai and Ward*, nutraceuticals production (for example of EPA) may likely be better derived directly from algae (as opposed to fish involving more extensive extraction processes and coming laden with other bioaccumulated toxins such as mercury). *P.t.* appears an excellent candidate species for sourcing EPA. Interestingly, there is evidence of a vitamin B_{12} control on EPA yield in *P.t.* as presented by *Yongmanitchai and Ward* [116]. Indeed in the larger context vitamin B_{12} is shown to play an important colimitation role in phytoplankton as described by *Bertrand et al.* [9].

With respect to future bio-production strategies it is important to carefully interpret results from batch-culture studies as presented here. Although the distinction of culture methods has been emphasized by some (example, *Siron et al.* [99]), it may easily be overlooked. Expansion on the topic of continuous production is presented in Appendix E.3.

3.3.6   Cell morphology and implications

During sample processing a significant note was the rapid filtration time for the urea treatment without nickel. Considering the silica draw-down observed, it would seem reasonable that the diatoms were forming more frustules which could help maintain open space across the filter membrane whereas cells with fewer or no frustules would tend towards filter clogging. This result has interesting implications when coupled with the lipid profiles and prospective industrial harvesting schemes; filtration could be more efficent depending on cell morphology (i.e., with frustules), but at the cost of reduced FAMEs (Figure 3.11, A), despite relatively un-compromised TLE (Figure 3.10).

3.4   Conclusions

Considering the comparison conditions (real world vs. laboratory) this study demonstrates a preliminary success of aggrandized bioproduction. Future work should yield continuous or semi-continuous chemostat systems which should greatly enhance production prospects with relatively minor added system complexity (automated growth monitoring, and fresh nutrient/medium supply at balance with withdrawn medium). Finally a finishing stage (open-pond) could be

incorporated for nutrient draw-down and lipid accumulation, thus forming a binary system which takes advantage of the best aspects of both closed and open system types.

When nickel is provided, urea is an an excellent nitrogen source for *P.t.* and yields quality FAMEs content with potential for both biofuels and nutraceuticals. Future work could begin to assess efficacy of municipal sewerage waste fractions as a nitrogen source – urea in this study was intended to simulate such an approach. Moreover, these results support the recent claim by *Yu et al.* that diatoms may represent an excellent choice for biofuel production, particularly in the light of their evidence (in the case of *T.p.*) that silica limitation may be more effective than nitrogen limitation in producing lipids amenable to fuel production.

Future proteomic assessment of samples collected across multiple growth stages from this study will better elucidate transcriptional regulation of lipid production perhaps making way for more effective production pathways as suggested by *Yu et al.* [117].

Finally, it can be determined from these results that TLE is not a "fool-proof" evaluation tool for prospecting microalgae strains as it is "blind" to the myriad component fatty acids which can have a variety of pros and cons as well as varying downstream processing and products. These results underscore the importance of detailed lipid profiling rather than simple TLE analysis (as is currently more prevalent in the literature) which perhaps falsely "justifies" certain strains or bioproduction methods over others.

Acknowledgments

Bibliography

[1] Air bp: Handbook of products, 2000.

[2] Annual energy review 2008, *Tech. Rep. DOE/EIA-0384(2008)*, U.S. Department of Energy, Energy Information Administration, Washington, DC 20585, 2009.

[3] Algal biofuels factsheet, *Tech. rep.*, United States Department of Energy, Biomass Program, 2009.

[4] Spot prices for crude oil and petroleum products, sourced online: January 10, 2010.

[5] Albentosa, M., A. Pérez-Camacho, U. Labarta, and M. J. Fernández-Reiriz, Evaluation of live microalgal diets for the seed culture of ruditapes decussatus using physiological and biochemical parameters, *Aquaculture*, *148*(1), 11–23, doi:DOI:10.1016/S0044-8486(96)01405-6, 1996.

[6] Atsumi, S., T. Hanai, and J. C. Liao, Non-fermentative pathways for synthesis of branched-chain higher alcohols as biofuels, *Nature*, *451*(7174), 86–89, 2008.

[7] Balat, M., M. Balat, E. KIrtay, and H. Balat, Main routes for the thermo-conversion of biomass into fuels and chemicals. part 2: Gasification systems, *Energy Conversion and Management*, *50*(12), 3158 – 3168, doi: DOI:10.1016/j.enconman.2009.08.013, 2009.

[8] Benini, S., W. R. Rypniewski, K. S. Wilson, S. Miletti, S. Ciurli, and S. Mangani, A new proposal for urease mechanism based on the crystal structures of the native and inhibited enzyme from bacillus pasteurii: why urea hydrolysis costs two nickels, *Structure*, *7*(2), 205–216, 1999.

[9] Bertrand, E. M., M. A. Saito, J. M. Rose, C. R. Riesselman, M. C. Lohan, A. E. Noble, P. A. Lee, and G. R. DiTullio, Vitamin b12 and iron colimi-

tation of phytoplankton growth in the ross sea, *Limnol. Oceanogr.*, *52*(3), 1079–1093, 2007.

[10] Bolton, J. R., Solar fuels: The production of energy-rich compounds by photochemical conversion and storage of solar energy, *Science*, *202*(4369), 705–711, 1978.

[11] Bolton, J. R., and D. . Hall, Photochemical conversion and storage of solar energy, *Anl. Rev. Ener*, *4*, 353–401, 1979.

[12] Bolton, J. R., S. J. Strickler, and J. S. Connolly, Limiting and realizable efficiencies of solar photolysis of water, *Nature*, *316*(6028), 495–500, 10.1038/316495a0 10.1038/316495a0, 1985.

[13] Bowler, C., et al., The phaeodactylum genome reveals the evolutionary history of diatom genomes, *Nature*, *456*(7219), 239–244, 2008.

[14] Carvalho, A. P., L. A. Meireles, and F. X. Malcata, Microalgal reactors: A review of enclosed system designs and performances, *Biotechnology Progress*, *22*(6), 1490–1506, 2006.

[15] Chisti, Y., Microalgae as sustainable cell factories, *Environmental Engineering and Management Journal*, *3*, 261–274, 2006.

[16] Chisti, Y., Biodiesel from microalgae, *Biotechnology Advances*, *25*, 294–306, 2007.

[17] Christie, W., A simple procedure for rapid transmethylation of glycerolipids and cholesteryl esters, *J. Lipid Res.*, *23*(7), 1072–1075, 1982.

[18] Cockerill, S., and C. Martin, Are biofuels sustainable? the eu perspective., *Biotechnology for biofuels*, *1*(1), 1–6, doi:10.1186/1754-6834-1-9, 2008.

[19] Conte, M. H., J. K. Volkman, and G. Eglinton, *The Haptophyta algae*, vol. 51, pp. 351–377, Clarendon Press, 1994.

[20] Conte, M. H., A. Thompson, D. Lesley, and R. P. Harris, Genetic and physiological influences on the alkenone/alkenoate versus growth temperature relationship in emiliania huxleyi and gephyrocapsa oceanica, *Geochimica et Cosmochimica Acta*, *62*(1), 51–68, doi:DOI:10.1016/S0016-7037(97)00327-X, 1998.

[21] Decker, J., Blooming biofuel: How algae could provide the solution, *Renewable Energy World Magazine*, *12*(3), 71–79, 2009.

[22] Doney, S. C., V. J. Fabry, R. A. Feely, and J. A. Kleypas, Ocean acidification: The other co2 problem, *Annual Review of Marine Science*, *1*(1), 169–192, doi:doi:10.1146/annurev.marine.010908.163834, 2009.

[23] Dupont, C. L., K. Barbeau, and B. Palenik, Ni uptake and limitation in marine synechococcus strains, *Appl. Environ. Microbiol.*, *74*(1), 23–31, doi:10.1128/AEM.01007-07, 2008.

[24] Eitinger, T., In vivo production of active nickel superoxide dismutase from prochlorococcus marinus mit9313 is dependent on its cognate peptidase, *J. Bacteriol.*, *186*(22), 7821–7825, doi:10.1128/JB.186.22.7821-7825. 2004, 2004.

[25] Eltgroth, M. L., R. L. Watwood, and G. V. Wolfe, Production and cellular localization of neutral long-chain lipids in the haptophyte algae <i>isochrysis galbana</i> and <i>emiliania huxleyi</i>¹, *Journal of Phycology*, *41*(5), 1000–1009, 2005.

[26] Enright, C., G. Newkirk, J. Craigie, and J. Castell, Evaluation of phytoplankton as diets for juvenile ostrea edulis l., *Journal of Experimental Marine Biology and Ecology*, *96*(1), 1–13, doi:DOI:10.1016/0022-0981(86)90009-2, 1986.

[27] Falkowski, P. G., R. T. Barber, and V. Smetacek, Biogeochemical controls and feedbacks on ocean primary production, *Science*, *281*(5374), 200–206, doi:10.1126/science.281.5374.200, 1998.

[28] Fargione, J., J. Hill, D. Tilman, S. Polasky, and P. Hawthorne, Land Clearing and the Biofuel Carbon Debt, *Science*, *319*(5867), 1235–1238, doi:10.1126/science.1152747, 2008.

[29] Fidalgo, J. P., A. Cid, E. Torres, A. Sukenik, and C. Herrero, Effects of nitrogen source and growth phase on proximate biochemical composition, lipid classes and fatty acid profile of the marine microalga isochrysis galbana, *Aquaculture*, *166*(1-2), 105–116, doi:DOI:10.1016/S0044-8486(98)00278-6, 1998.

[30] Field, C. B., M. J. Behrenfeld, J. T. Randerson, and P. Falkowski, Primary production of the biosphere: Integrating terrestrial and oceanic components, *Science*, *281*(5374), 237–240, doi:10.1126/science.281.5374.237, 1998.

[31] Firme, G. F., E. L. Rue, D. A. Weeks, K. W. Bruland, and D. A. Hutchins, Spatial and temporal variability in phytoplankton iron limitation along the

california coast and consequences for si, n, and c biogeochemistry, *Global Biogeochem. Cycles*, *17*, 2003.

[32] Frentzen, M., and F. Wolter, *Molecular biology of acyltransferases involved in glycerolipid synthesis*, chap. 10, pp. 247–272, Cambridge University Press, 1998.

[33] Girisuta, B., Untitled, chapter 1, Ph.D. thesis, 2007.

[34] Gressel, J., Transgenics are imperative for biofuel crops, *Plant Science*, *174*(3), 246–263, doi:DOI:10.1016/j.plantsci.2007.11.009, 2008.

[35] Griffiths, M., and S. Harrison, Lipid productivity as a key characteristic for choosing algal species for biodiesel production, *Journal of Applied Phycology*, doi:10.1007/s10811-008-9392-7, 2009.

[36] Guillard, R., *Culture of phytoplankton for feeding marine invertebrates in "Culture of Marine Invertebrate Animals."*, pp. 26–60, Plenum Press, New York, USA, in "Culture of Marine Invertebrate Animals.", 1975.

[37] Guillard, R., and J. Ryther, Studies of marine planktonic diatoms. i. cyclotella nana hustedt and detonula confervacea cleve., *Can. J. Microbiol.*, *8*, 229–239, 1962.

[38] Haiduc, A., M. Brandenberger, S. Suquet, F. Vogel, R. Bernier-Latmani, and C. Ludwig, Sunchem: an integrated process for the hydrothermal production of methane from microalgae and co2 mitigation, *Journal of Applied Phycology*, *21*, 529–541, doi:10.1007/s10811-009-9403-3, 2009.

[39] Hemschemeier, A., A. Melis, and T. Happe, Analytical approaches to photobiological hydrogen production in unicellular green algae, *Photosynthesis Research*, doi:10.1007/s11120-009-9415-5, 2009.

[40] Hill, J., E. Nelson, D. Tilman, S. Polasky, and D. Tiffany, Environmental, economic, and energetic costs and benefits of biodiesel and ethanol biofuels, *Proceedings of the National Academy of Sciences*, *103*(30), 11,206–11,210, doi:10.1073/pnas.0604600103, 2006.

[41] Hirsch, R. L., R. Bezdek, and R. Wendling, Peaking of world oil production: impacts, mitigation, & risk management, *Tech. rep.*, National Energy Technology Laboratory, 2005.

[42] Hoegh-Guldberg, O., et al., Coral reefs under rapid climate change and ocean acidification, *Science*, *318*(5857), 1737–1742, doi:10.1126/science.1152509, 2007.

[43] Hu, Q., M. Sommerfeld, E. Jarvis, M. Ghirardi, M. Posewitz, M. Seibert, and A. Darzins, Microalgal triacylglycerols as feedstocks for biofuel production: perspectives and advances, *The Plant Journal: For Cell and Molecular Biology*, *54*(4), 621–39, 2008.

[44] Huntley, M., and D. Redalje, Co2 mitigation and renewable oil from photosynthetic microbes: A new appraisal, *Mitigation and Adaptation Strategies for Global Change*, *12*(4), 573–608, doi:10.1007/s11027-006-7304-1, 2007.

[45] Imahara, H., E. Minami, and S. Saka, Thermodynamic study on cloud point of biodiesel with its fatty acid composition, *Fuel*, *85*(12-13), 1666–1670, doi:DOI:10.1016/j.fuel.2006.03.003, 2006.

[46] Inderwildi, O. R., and D. A. King, Quo vadis biofuels?, *Energy & Environmental Science*, *2*, 343–346, doi:DOI:10.1039/b822951c, 2009.

[47] IPCC, Publications and data, in *The IPCC Assessment Reports*, IPCC, 2009.

[48] Jones, N., Sneak test shows positive-paper bias, *Nature*, doi:doi:10.1038/news.2009.914, published online 14 September 2009, 2009.

[49] Kaplan, D., A. Richmond, Z. Dubinsky, and S. Aaronson, *Handbook of Microalgal Mass Culture: Algal nutrition*, pp. 147–198, CRC Press, FL, 1986.

[50] Kaur, S., H. K. Gogoi, R. B. Srivastava, and M. C. Kalita, Algal diversity as a renewable feedstock for biodiesel, *Current Science*, *96*(2), 182, 2009.

[51] Kerschbaum, S., G. Rinke, and K. Schubert, Winterization of biodiesel by micro process engineering, *Fuel*, *87*(12), 2590 – 2597, doi:DOI:10.1016/j.fuel.2008.01.023, 2008.

[52] Knoshaug, E. P., R. Sestric, E. Jarvis, Y.-C. Chou, P. T. Pienkos, and A. Darzins, Current status of the department of energy's aquatic species program lipid-focused algae collection, presented at the 31st Symposium on Biotechnology for Fuels and Chemicals, 2009.

[53] Knothe, G., "designer" biodiesel: optimizing fatty ester composition to improve fuel properties, *Energy & Fuels*, *22*, 1358–1364, 2008.

[54] Knothe, G., Biodiesel and renewable diesel: A comparison, *Progress in Energy and Combustion Science*, *In Press, Corrected Proof*, doi:DOI:10.1016/j.pecs.2009.11.004, 2009.

[55] Lapola, D. M., R. Schaldach, J. Alcamo, A. Bondeau, J. Koch, C. Koelking, and J. A. Priess, Indirect land-use changes can overcome carbon savings from biofuels in brazil, *Proceedings of the National Academy of Sciences*, doi:10.1073/pnas.0907318107, 2010.

[56] Lavens, P., and P. Sorgeloos, Manual on the production and use of live food for aquaculture, *Fisheries Technical Paper 361*, Food and Agriculture Organization of the United Nations, section 2.5. Use of micro-algae in aquaculture (p 36), 1996.

[57] Lebeau, T., and J.-M. Robert, Diatom cultivation and biotechnologically relevant products. part ii: Current and putative products, *Applied Microbiology and Biotechnology*, *60*, 624–632, 2002.

[58] Li, Y., M. Horsman, N. Wu, C. Q. Lan, and N. Dubois-Calero, Biofuels from microalgae, *Biotechnology Progress*, *24*(4), 815–820, 2008.

[59] Litos Strategic, C., The smart grid: An introduction, prepared for the U.S. Department of Energy under contract No. DE-AC26-04NT41817, Subtask 560.01.04., 2008.

[60] Lynd, L. R., J. H. Cushman, R. J. Nichols, and C. E. Wyman, Fuel Ethanol from Cellulosic Biomass, *Science*, *251*(4999), 1318–1323, doi:10.1126/science.251.4999.1318, 1991.

[61] Madrigal, A., How algal biofuels lost a decade in the race to replace oil, sourced online (18 January 2010), 2009.

[62] Mann, J. E., and J. Myers, On pigments, growth, and photosynthesis of <i>phaeodactylum tricornutum</i>, *Journal of Phycology*, *4*(4), 349–355, 1968.

[63] Marchler-Bauer, A., et al., Cdd: a conserved domain database for protein classification, *Nucl. Acids Res.*, *33*, 192–196, doi:10.1093/nar/gki069, 2005.

[64] Marlowe, I. T., J. C. Green, A. C. Neal, S. C. Brassell, G. Eglinton, and P. A. Course, Long chain (n-c37-c39) alkenones in the prymnesiophyceae. distribution of alkenones and other lipids and their taxonomic significance, *European Journal of Phycology*, *19*(3), 203–216, 1984.

[65] Mata, T. M., A. A. Martins, and N. S. Caetano, Microalgae for biodiesel production and other applications: A review, *Renewable and Sustainable Energy Reviews*, *14*(1), 217–232, doi:DOI:10.1016/j.rser.2009.07.020, 2010.

[66] Metzler, D. E., and C. M. Metzler, *Light and life*, vol. 2, chap. 23, pp. 1272–1357, Academic Press, 2003.

[67] Middelburg, J. J., and F. J. R. Meysman, Ocean science: Burial at sea, *Science*, *316*(5829), 1294–1295, doi:10.1126/science.1144001, 2007.

[68] Mirón, A. S., A. C. Gómez, F. G. Camacho, E. M. Grima, and Y. Chisti, Comparative evaluation of compact photobioreactors for large-scale monoculture of microalgae, *Journal of Biotechnology*, *70*(1-3), 249–270, doi:DOI:10.1016/S0168-1656(99)00079-6, biotechnological Aspects of Marine Sponges, 1999.

[69] Mohr, H., and P. Schopfer, *C4 Plants and CAM Plants*, p. 253, Springer, 1995.

[70] Montsant, A., K. Jabbari, U. Maheswari, and C. Bowler, Comparative genomics of the pennate diatom phaeodactylum tricornutum, *Plant Physiol.*, *137*(2), 500–513, doi:10.1104/pp.104.052829, 2005.

[71] Moser, B., Biodiesel production, properties, and feedstocks, *In Vitro Cellular & Developmental Biology - Plant*, *45*, 229–266, doi:10.1007/s11627-009-9204-z, 2009.

[72] Moynihan, M., Plankton power and rtdc announce proposed algae-to-biofuels pilot facility on cape cod, Online (3 August 2009), 2009.

[73] NREL, Algal-derived oil feedstock research at nrel: Beyond the doe's aquatic species program, in *Presented at the fifth meeting of the Asia-Pacific Economic Cooperation (APEC) Task Force*, Golden, Colorado., 2008.

[74] O'Neil, G. W., D. J. Moser, and E. O. Volz, Metathesis reactions of [beta]-acyloxysulfones: synthesis of 1,6- and 1,7-dienes, *Tetrahedron Letters*, *50*(52), 7355–7357, doi:DOI:10.1016/j.tetlet.2009.10.071, 2009.

[75] Patterson, G., L. Larsen, and R. Moore, Bioactive natural products from blue-green algae, *Journal of Applied Phycology*, *6*(2), 151–157, 1994.

[76] Patterson, G., E. Tsitsa-Tsardis, G. Wikfors, P. Gladu, D. Chitwood, and D. Harrison, Sterols and alkenones of isochrysis, *Phytochemistry*, *35*(5), 1233–1236, doi:DOI:10.1016/S0031-9422(00)94826-X, 1994.

[77] Petrou, E. C., and C. P. Pappis, Biofuels: A survey on pros and cons, *Energy & Fuels*, *23*(2), 1055–1066, doi:10.1021/ef800806g, 2009.

[78] Pokhodenko, V. D., and V. V. Pavlishchuk, Green chemistry and modern technology, *Theoretical and Experimental Chemistry*, *38*(2), 69–87, 2002.

[79] Price, N. M., and F. M. M. Morel, Colimitation of phytoplankton growth by nickel and nitrogen, *Limnology and Oceanography*, *36*(6), 1071–1077, 1991.

[80] Rechka, J., and J. Maxwell, Characterisation of alkenone temperature indicators in sediments and organisms, *Organic Geochemistry*, *13*(4-6), 727–734, doi:DOI:10.1016/0146-6380(88)90094-0, proceedings of the 13th International Meeting on Organic Geochemistry, 1988.

[81] Rechka, J. A., and J. R. Maxwell, Unusual long chain ketones of algal origin, *Tetrahedron Letters*, *29*, 2599–2600, 1988.

[82] Rees, T. A. V., and I. A. Bekheet, The role of nickel in urea assimilation by algae, *Planta*, *156*(5), 385–387, 1982.

[83] Rees, T. A. V., and P. J. Syrett, The uptake of urea by the diatom, phaeodactylum, *New Phytologist*, *82*(1), 169–178, 1979.

[84] Roberts, K., E. Granum, R. C. Leegood, and J. A. Raven, C3 and c4 pathways of photosynthetic carbon assimilation in marine diatoms are under genetic, not environmental, control, *Plant Physiol.*, *145*(1), 230–235, doi: 10.1104/pp.107.102616, 2007.

[85] Rodolfi, L., G. C. Zittelli, N. Bassi, G. Padovani, N. Biondi, G. Bonini, and M. R. Tredici, Microalgae for oil: Strain selection, induction of lipid synthesis and outdoor mass cultivation in a low-cost photobioreactor, *Biotechnology and Bioengineering*, *102*(1), 100–112, 2009.

[86] Rontani, J.-F., D. Marchand, and J. K. Volkman, Nabh4 reduction of alkenones to the corresponding alkenols: a useful tool for their characterisation in natural samples, *Organic Geochemistry*, *32*(11), 1329–1341, doi:DOI:10.1016/S0146-6380(01)00091-2, 2001.

[87] Rontani, J.-F., F. G. Prahl, and J. K. Volkman, Re-examinatino of the double bond positions in alkenones and derivatives: biosynthetic implications, *Journal of Phycology*, *42*(4), 800–813, 2006.

[88] Rosa, L. P., C. P. de Campos, and M. S. M. de Araujo, Biofuel contribution to mitigate fossil fuel co[sub 2] emissions: Comparing sugar cane ethanol in brazil with corn ethanol and discussing land use for food production and deforestation, *Journal of Renewable and Sustainable Energy*, *1*(3), 033111, doi:10.1063/1.3139803, 2009.

[89] Saito, M. A., and T. J. Goepfert, Zinc-cobalt colimitation of phaeocystis antarctica, *Limnol. Oceanogr.*, *53*, 266–275, 2008.

[90] Saito, M. A., T. J. Goepfert, and J. T. Ritt, Some thoughts on the concept of colimitation: Three definitions and the importance of bioavailability, *Limnol. Oceanogr.*, *53*(1), 276–290, 2008.

[91] Schueneman, T., Algae biofuel: Hype, hope, and promise, 2009.

[92] Searchinger, T., R. Heimlich, R. A. Houghton, F. Dong, A. Elobeid, J. Fabiosa, S. Tokgoz, D. Hayes, and T.-H. Yu, Use of u.s. croplands for biofuels increases greenhouse gases through emissions from land use change, *Science*, *319*, 1238–1240, 2008.

[93] Service, R. F., Biofuels: Eyeing oil, synthetic biologists mine microbes for black gold, *Science*, *322*(5901), 522–523, doi:10.1126/science.322.5901. 522, 2008.

[94] Service, R. F., ExxonMobil Fuels Venter's Efforts To Run Vehicles on Algae-Based Oil, *Science*, *325*(5939), 379, doi:10.1126/science.325_379a, 2009.

[95] Sheehan, J., T. Dunahay, J. Benemann, and P. Roessler, National renewable energy laboratories - biomass energy: A look back at the u.s. department of energy's aquatic species program: Biodiesel from algae close-out report, *Tech. Rep. NREL/TP-580-24190*, National Renewable Energy Laboratories, 1998.

[96] Sheehan, J. J., Biofuels and the conundrum of sustainability., *Current opinion in biotechnology*, doi:10.1016/j.copbio.2009.05.010, 2009.

[97] Shockley, W., and H. J. Queisser, Detailed balance limit of efficiency of p-n junction solar cells, *Journal of Applied Physics*, *32*(3), 510–519, 1961.

[98] Sirko, A., and R. Brodzik, Plant ureases: Roles and regulation, *Acta Biochemica Polonica*, *47*(4), 1189–1195, 2000.

[99] Siron, R., G. Giusti, and B. Berland, Changes in the fatty acid composition of phaeodactylum tricornutum and dunaliella tertiolecta during growth and under phosphorus deficiency., *Marine ecology progress series*, *55*(1), 95–100, 1989.

[100] Soeder, C. J., and G. Engelmann, Nickel requirement in chlorella emersonii, *Archives of Microbiology*, *137*(1), 85–87, 1984.

[101] Stewart, R. R., *Our Ocean Planet: Oceanography in the 21st Century*, chap. Marine Fisheries Food Webs, Dept. of Oceanography, Texas A&M University, 2005.

[102] Stipp, D., The next big thing in energy: Pond scum?, sourced online (10 January 2010), 2008.

[103] Stucki, S., F. Vogel, C. Ludwig, A. G. Haiduc, and M. Brandenberger, Catalytic gasification of algae in supercritical water for biofuel production and carbon capture, *Energy & Environmental Science*, 2, 535–541, doi: DOI:10.1039/b819874h, 2009.

[104] Taiz, L., and E. Zeiger, *Plant Physiology*, 4 ed., 705 pp., Lincoln Taiz and Eduardo Zeiger, 2006.

[105] Todd, M. J., and R. P. Hausinger, Purification and characterization of the nickel-containing multicomponent urease from klebsiella aerogenes., *Journal of Biological Chemistry*, 262(13), 5963–5967, 1987.

[106] Uduman, N., Y. Qi, M. K. Danquah, G. M. Forde, and A. Hoadley, Dewatering of microalgal cultures: A major bottleneck to algae-based fuels, *Journal of Renewable and Sustainable Energy*, 2(1), 012,701, 2010.

[107] Volkman, J. K., S. M. Barrerr, S. I. Blackburn, and E. L. Sikes, Alkenones in gephyrocapsa oceanica: Implications for studies of paleoclimate, *Geochimica et Cosmochimica Acta*, 59(3), 513–520, doi:DOI:10.1016/ 0016-7037(95)00325-T, 1995.

[108] Waldron, K. J., and N. J. Robinson, How do bacterial cells ensure that metalloproteins get the correct metal?, *Nat Rev Micro*, 7(1), 25–35, 2009.

[109] Waltz, E., Battlefield: Papers suggesting that biotech crops might harm the environment attract a hail of abuse from other scientists., *Nature*, 461(3), 27–32, doi:10.1038/461027a, 2009.

[110] Wang, B., Y. Li, N. Wu, and C. Q. Lan, Co2 bio-mitigation using microalgae, *Applied Microbiology and Biotechnology*, 79(5), 707–718, doi: 10.1007/s00253-008-1518-y, 2008.

[111] Westbrook, S. R., and R. LeCren, *Fuels and lubricants handbook: technology, properties, performance, and testing*, chap. 5, ASTM International, (pp 121-2), 2003.

[112] Wikfors, G. H., and G. W. Patterson, Differences in strains of isochrysis of importance to mariculture, *Aquaculture*, *123*(1-2), 127–135, doi:DOI: 10.1016/0044-8486(94)90125-2, 1994.

[113] Wu, Q., J. Dai, Y. Shiraiwa, G. Sheng, and J. Fu, A renewable energy source - hydrocarbon gases resulting from pyrolysis of the marine nanoplanktonic alga emiliania huxleyi, *Journal of Applied Phycology*, *11*(2), 137–142, 1999.

[114] Wu, Q., W. Ruiyong, D. Junbiao, S. Yitao, and Y. Shiraiwa, Hydrocarbons pyrolysed from nannoplanktonic algae: An experimental organism system for study on the origin of petroleum and natural gas, *Chinese Science Bulletin*, *44*, 767–768, 1999.

[115] Ye, X., Y. Wang, R. Hopkins, M. W. Adams, B. Evans, J. Mielenz, and Y.-H. P. Zhang, Spontaneous high-yield production of hydrogen from cellulosic materials and water catalyzed by enzyme cocktails, *ChemSusChem*, *2*, 149–152, 2009.

[116] Yongmanitchai, W., and P. Ward, Growth of and omega-3 fatty acid production by phaeodactylum tricornutum under different culture conditions, *Applied and Environmental Microbiology*, *57*, 419–425, 1991.

[117] Yu, E., F. Zendejas, P. Lane, S. Gaucher, B. Simmons, and T. Lane, Triacylglycerol accumulation and profiling in the model diatoms thalassiosira pseudonana and phaeodactylum tricornutum (baccilariophyceae) during starvation, *Journal of Applied Phycology*, *21*(6), 669–681, 2009.

[118] Yuksel, A., H. Koga, M. Sasaki, and M. Goto, Electrolysis of glycerol in subcritical water, *Journal of Renewable and Sustainable Energy*, *1*(3), 033112, doi:10.1063/1.3156006, 2009.

[119] Zhou, N., and M. A. McNeil, Assessment of historic trend in mobility and energy use in india transportation sector using bottom-up approach, *Journal of Renewable and Sustainable Energy*, *1*(4), 043108, doi:10.1063/1.3156008, 2009.

Appendix A

Appendix organization, nomenclature, and glossary

"WHOI's role in biofuels could be like that of the shovel salesman during the gold rush in the wild-west"

- Tracy Mincer, Assistant Scientist, WHOI; referring to the role of WHOI in technology transfer and R&D for the emerging and potentially very lucrative microalgal biofuels movement.

Organization

Supplemental materials in the following appendices are generally sectioned to coordinate with the chapters of the main text, for example, Appendix B supports Chapter 2, while Appendix C supports Chapter 3. Remaining appendices support the work more generally. Foremost, however is the following nomenclature list and glossary.

Nomenclature / Glossary

ASP Aquatic Species Program, a nearly two decade long research endeavor (1978-1996) funded by the United States Department of Energy. The ASP researched energy production using algae, particularly in inexpensive open-pond cultures.

ASTM American Society for Testing and Materials

B100 Biodiesel (100 percent), similarly, B10 is 10 percent biodiesel with 90 percent fossil diesel an so on with B20, B50, etc.

BHT Butylated hydroxytoluene

BLAST Basic local allignment search tool, a web-based graphical user interface for genomic and proteomic sequence allignment.

C17 n-heptadecane (also nC17)

C19 Nonadecanoate

CCMP Center for Culture of Marine Phytoplankton

CP Cloud point

DOE Department of Energy (United States)

EPA Eicosapentaenoic acid (also icosapentaenoic acid), an omega-3 fatty acid.

FAEE Fatty acid ethyl ester

FAME Fatty acid methyl ester

FID Flame ionization detector

GC Gas chromatograph

ha   Hectare, unit of area equal to 10,000 square meters.

IMG   Integrated Microbial Genomes, a community resource for comparative analysis and annotation of all publicly available genomes from three domains of life in a uniquely integrated context.

IPCC   Intergovernmental Panel on Climate Change

IRF   Internal response factor

JGI   Joint Genome Institute

kWh   Kilowatt-hour, a unit of energy which can be converted to MJ where 1 kWh = 3.6 MJ.

MBL   Marine Biological Laboratory

MJ   Mega Joule, a unit of energy which can be converted to kWh where 1 MJ is approximately 0.278 kWh.

MOP   Methylated oil product

MRC   Marine Resource Center (section of the Marine Biological Laboratories)

NCBI   National Center for Biotechnology Information, (http://www.ncbi.nlm.nih.gov)

NiSOD   Nickel dependent superoxide dismutase

NOAA   National Oceanic and Atmospheric Administration

P.t.   Phaeodactylum tricornutum

PAR   Photosynthetically active radiation

PBR   Photobioreactor, a cultivation system designed for batch or chemostat culturing of photosynthetic organisms (eg. algae).

PULCA   Polyunsaturated long-chain (mainly C37-38) alkenones

RFU   Relative fluoresensce units

SOD   Superoxide dismutase

T.p.   Thalassiosira pseudonana

TAG   Triacylglycerol

TLE   Total lipid extract

TOC   Total organic carbon

UHP   Ultra high purity

WHOI Woods Hole Oceanographic Institution

Appendix B

Supplement to Chapter 2

The results of Chapter 2 have been prepared and submitted in similar form to *Energy & Environmental Science* where they are in peer review for publication as a correspondence (submitted January 2010).

B.1   GC-FID methods

GC-FID method details are identical to those outlined in Appendix C.3.

Appendix C

*S*upplement to Chapter 3

C.1   Molecular background to experiment

As background to the urease and nickel experiments with *P.t.*, it was both relevant and necessary to gather some current basic genomic information such as is easily obtained with online database resources (e.g.. JGI, IMG, and NCBI). In this case NCBI and it's associated tools, "BLAST" and "BLink" was used as a reference tool for the nickel-urease protein search and comparison. Example results of the conserved domain urease α-subunit are presented in Figure C.1.
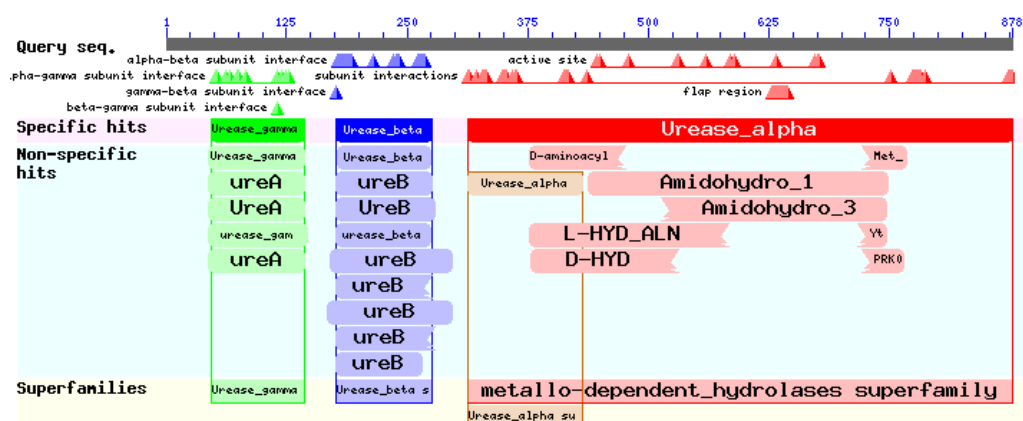
Figure C.1: Graphical interface results in NCBI for predicted protein including the urease α-subunit, Phaeodactylum tricornutum CCAP 1055/1.

C.2 GC-FID chromatograms and integration results

The following figures are organized uniformly and systematically to detail the raw source data used to determine lipid profiles as presented in Section 3.3. The example Figure C.2 identifies the peak numbers (in parenthesis), retention times (x-axis), and integrated peak areas (above peaks) as were integrated and quantified for all similar figures. Table C.1 contains relevant compounds quantified and the approximate retention times.

Beginning with Figure C.3, subsequent presentation alternates between chromatograms and integration data summary tables for 4 time-points, days 2, 4, 6, 9; early, mid, late- exponential, and "stationary" phases respectively.
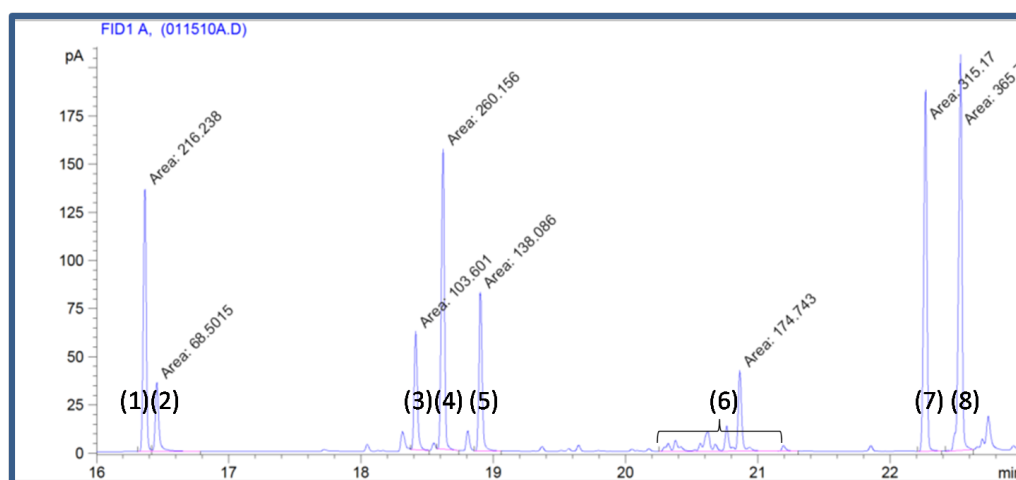
Figure C.2: Example Chromatogram with peaks as specified in Table C.1.

Peak #	Approximate retention time (minutes)	Compound (typical nomenclature is C:D, where C = carbon length, D = double bonds)
1	16.4	17:0, nC17 Alkane (external standard)
2	16.5	14:0
3	18.4	16:2 (assumed)
4	18.6	16:1
5	18.9	16:0
6	20.9	All 18s
7	22.3	C19 FAME (internal standard)
8	22.5	20:5 (EPA)

Table C.1: Compounds, retention time, and peak number typical of these GC-FID results.

Figure C.3: Day 2 (early exponential phase) chromatograms for replete (top), +Urea,-Ni (middle), and+Urea,+Ni (bottom) samples

```
========================================================================
                          Integration Results
========================================================================

Signal 1: FID1 A,   (011410B.D)


Peak    Time    Type       Area          Height      Width     Start       End
  #     [min]            [pA*s]           [pA]        [min]     [min]       [min]
----|--------|----|------------|------------|-------|--------|--------|
   1   16.365 MF      249.71642     152.19992   0.0273   16.318    16.443
   2   16.476 FM       13.33134       4.95376   0.0449   16.443    16.626
   3   18.622 MM       39.13775      19.28872   0.0338   18.579    18.776
   4   18.904 MM       54.20449      28.45411   0.0317   18.866    19.114
   5   20.870 MM       32.62444       2.90718   0.1870   20.269    21.333
   6   22.264 MM      324.13611     171.06451   0.0316   22.207    22.462
   7   22.525 MM       17.99994       8.34263   0.0360   22.488    22.738


Signal 2: FID1 A,   (011410C.D)


Peak    Time    Type       Area          Height      Width     Start       End
  #     [min]            [pA*s]           [pA]        [min]     [min]       [min]
----|--------|----|------------|------------|-------|--------|--------|
   1   16.364 MF      235.04382     140.00136   0.0280   16.320    16.443
   2   16.472 FM       14.03810       5.39193   0.0434   16.443    16.614
   3   18.617 MM       43.15258      21.52684   0.0334   18.578    18.774
   4   18.905 MM       47.84972      25.36442   0.0314   18.864    19.122
   5   20.864 MM       65.85972      16.46505   0.0667   20.249    21.358
   6   22.262 MM      285.60089     150.00868   0.0317   22.201    22.468
   7   22.525 MM       15.14304       6.83167   0.0369   22.485    22.721


Signal 3: FID1 A,   (011410D.D)


Peak    Time    Type       Area          Height      Width     Start       End
  #     [min]            [pA*s]           [pA]        [min]     [min]       [min]
----|--------|----|------------|------------|-------|--------|--------|
   1   16.363 MF      240.11299     143.33037   0.0279   16.318    16.447
   2   16.478 FM       11.89063       4.02520   0.0492   16.447    16.625
   3   18.620 MM       37.92977      18.84645   0.0335   18.580    18.782
   4   18.904 MM       43.31629      21.48145   0.0336   18.866    19.086
   5   20.874 MM       23.41491       1.57762   0.2474   20.252    21.320
   6   22.260 MM      287.09991     141.05292   0.0339   22.204    22.474
   7   22.524 MM       12.84224       5.80946   0.0368   22.482    22.705


========================================================================
```

Table C.2: Day 2 (early exponential phase) integration results for replete (top), +Urea,-Ni (middle), and+Urea,+Ni (bottom) samples
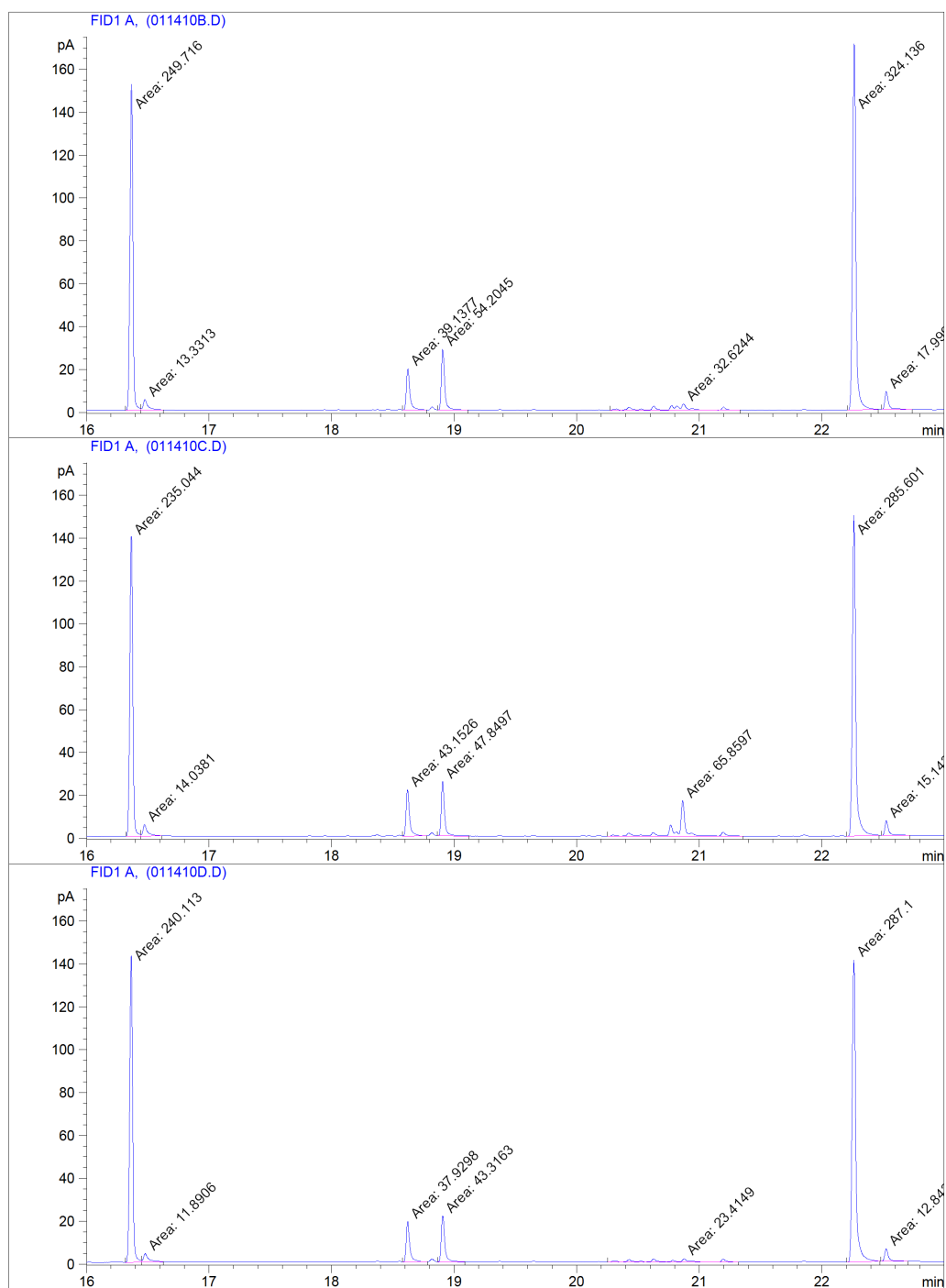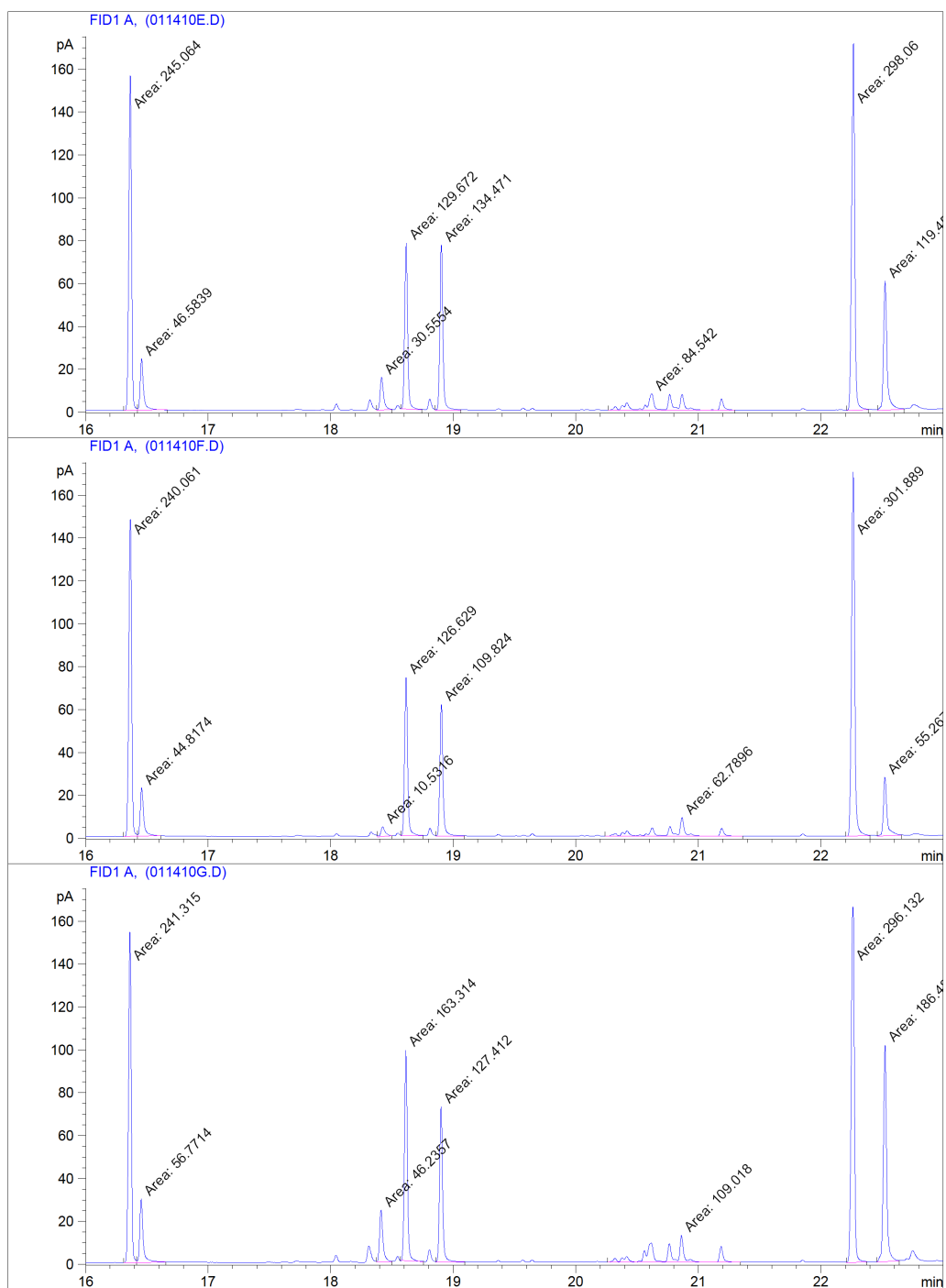
Figure C.4: Day 4 (mid-exponential phase) chromatograms for replete (top), +Urea,-Ni (middle), and +Urea,+Ni (bottom) samples

```
=======================================================================
                         Integration Results
=======================================================================

Signal 1: FID1 A,   (011410E.D)


Peak    Time    Type     Area        Height     Width    Start     End
 #      [min]           [pA*s]        [pA]      [min]    [min]    [min]
----|--------|----|-----------|-----------|-------|--------|--------|
   1   16.363 MF    245.06357   156.46091  0.0261   16.310   16.422
   2   16.454 FM     46.58392    23.95892  0.0324   16.422   16.665
   3   18.414 MM     30.55543    15.31558  0.0333   18.375   18.502
   4   18.615 MM    129.67169    77.56647  0.0279   18.571   18.744
   5   18.901 MM    134.47144    77.18136  0.0290   18.853   19.063
   6   20.617 MM     84.54195     7.69279  0.1832   20.263   21.299
   7   22.265 MM    298.06039   171.36748  0.0290   22.211   22.386
   8   22.523 MM    119.45525    60.24854  0.0330   22.464   22.680


Signal 2: FID1 A,   (011410F.D)


Peak    Time    Type     Area        Height     Width    Start     End
 #      [min]           [pA*s]        [pA]      [min]    [min]    [min]
----|--------|----|-----------|-----------|-------|--------|--------|
   1   16.364 MF    240.06088   147.78317  0.0271   16.307   16.423
   2   16.455 FM     44.81740    22.49771  0.0332   16.423   16.613
   3   18.422 MM     10.53158     4.56613  0.0384   18.383   18.501
   4   18.613 MM    126.62918    74.04644  0.0285   18.572   18.755
   5   18.903 MM    109.82397    61.63587  0.0297   18.859   19.090
   6   20.868 MM     62.78961     8.66590  0.1208   20.240   21.362
   7   22.264 MM    301.88858   170.04216  0.0296   22.205   22.402
   8   22.521 MM     55.26760    27.26020  0.0338   22.460   22.657


Signal 3: FID1 A,   (011410G.D)


Peak    Time    Type     Area        Height     Width    Start     End
 #      [min]           [pA*s]        [pA]      [min]    [min]    [min]
----|--------|----|-----------|-----------|-------|--------|--------|
   1   16.360 MF    241.31505   154.57751  0.0260   16.310   16.418
   2   16.452 FM     56.77140    29.66251  0.0319   16.418   16.655
   3   18.411 MM     46.23574    24.17266  0.0319   18.372   18.501
   4   18.612 MM    163.31430    98.33035  0.0277   18.569   18.757
   5   18.899 MM    127.41245    72.66513  0.0292   18.859   19.093
   6   20.861 MM    109.01830    12.58395  0.1444   20.258   21.344
   7   22.260 MM    296.13202   166.14421  0.0297   22.208   22.377
   8   22.524 MM    186.48080   101.12325  0.0307   22.458   22.639


=======================================================================
```

Table C.3: Day 4 (mid-exponential phase) integration results for replete (top), +Urea,-Ni (middle), and+Urea,+Ni (bottom) samples
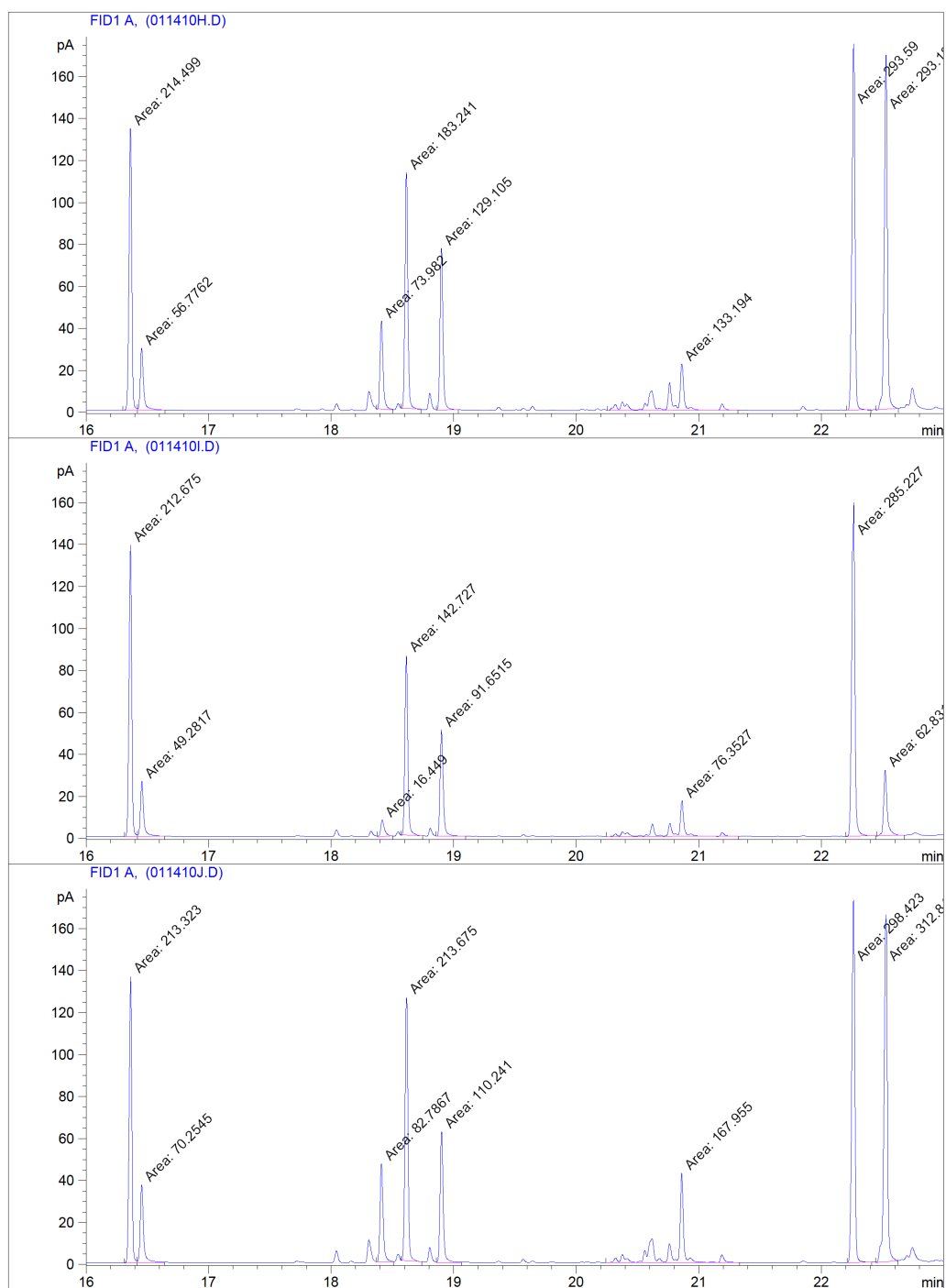
Figure C.5: Day 6 (late exponential phase) chromatograms for replete (top), +Urea,-Ni (middle), and+Urea,+Ni (bottom) samples

```
========================================================================
                           Integration Results
========================================================================


Signal 1: FID1 A,   (011410H.D)


Peak   Time    Type     Area        Height      Width    Start     End
  #    [min]           [pA*s]        [pA]       [min]     [min]    [min]
----|--------|----|-----------|-----------|-------|--------|--------|
   1   16.360 MF      214.49913   134.33727   0.0266   16.301   16.419
   2   16.452 FM       56.77623    29.63540   0.0319   16.419   16.646
   3   18.410 MM       73.98199    42.01004   0.0294   18.372   18.505
   4   18.613 MM      183.24052   112.48692   0.0271   18.572   18.732
   5   18.899 MM      129.10530    77.05485   0.0279   18.859   19.038
   6   20.861 MM      133.19411    21.98823   0.1010   20.257   21.320
   7   22.262 MM      293.58987   174.90157   0.0280   22.205   22.405
   8   22.528 MM      293.18271   169.43721   0.0288   22.446   22.628


Signal 2: FID1 A,   (011410I.D)


Peak   Time    Type     Area        Height      Width    Start     End
  #    [min]           [pA*s]        [pA]       [min]     [min]    [min]
----|--------|----|-----------|-----------|-------|--------|--------|
   1   16.362 MF      212.67509   139.02036   0.0255   16.313   16.420
   2   16.455 FM       49.28172    26.16410   0.0314   16.420   16.641
   3   18.416 MM       16.44902     7.84382   0.0350   18.379   18.503
   4   18.613 MM      142.72653    85.75709   0.0277   18.572   18.749
   5   18.899 MM       91.65153    50.73474   0.0301   18.855   19.098
   6   20.864 MM       76.35272    16.93621   0.0751   20.247   21.322
   7   22.264 MM      285.22665   159.47592   0.0298   22.202   22.444
   8   22.521 MM       62.83119    31.32696   0.0334   22.453   22.678


Signal 3: FID1 A,   (011410J.D)


Peak   Time    Type     Area        Height      Width    Start     End
  #    [min]           [pA*s]        [pA]       [min]     [min]    [min]
----|--------|----|-----------|-----------|-------|--------|--------|
   1   16.362 MF      213.32271   136.65379   0.0260   16.312   16.417
   2   16.452 FM       70.25454    37.13921   0.0315   16.417   16.641
   3   18.410 MM       82.78673    46.75909   0.0295   18.371   18.508
   4   18.614 MM      213.67465   125.60513   0.0284   18.571   18.741
   5   18.901 MM      110.24146    62.44361   0.0294   18.860   19.064
   6   20.860 MM      167.95508    42.62908   0.0657   20.242   21.333
   7   22.261 MM      298.42313   172.86929   0.0288   22.212   22.413
   8   22.526 MM      312.84546   165.60692   0.0315   22.445   22.627


========================================================================
```

Table C.4: Day 6 (late-exponential phase) integration results for replete (top), +Urea,-Ni (middle), and+Urea,+Ni (bottom) samples

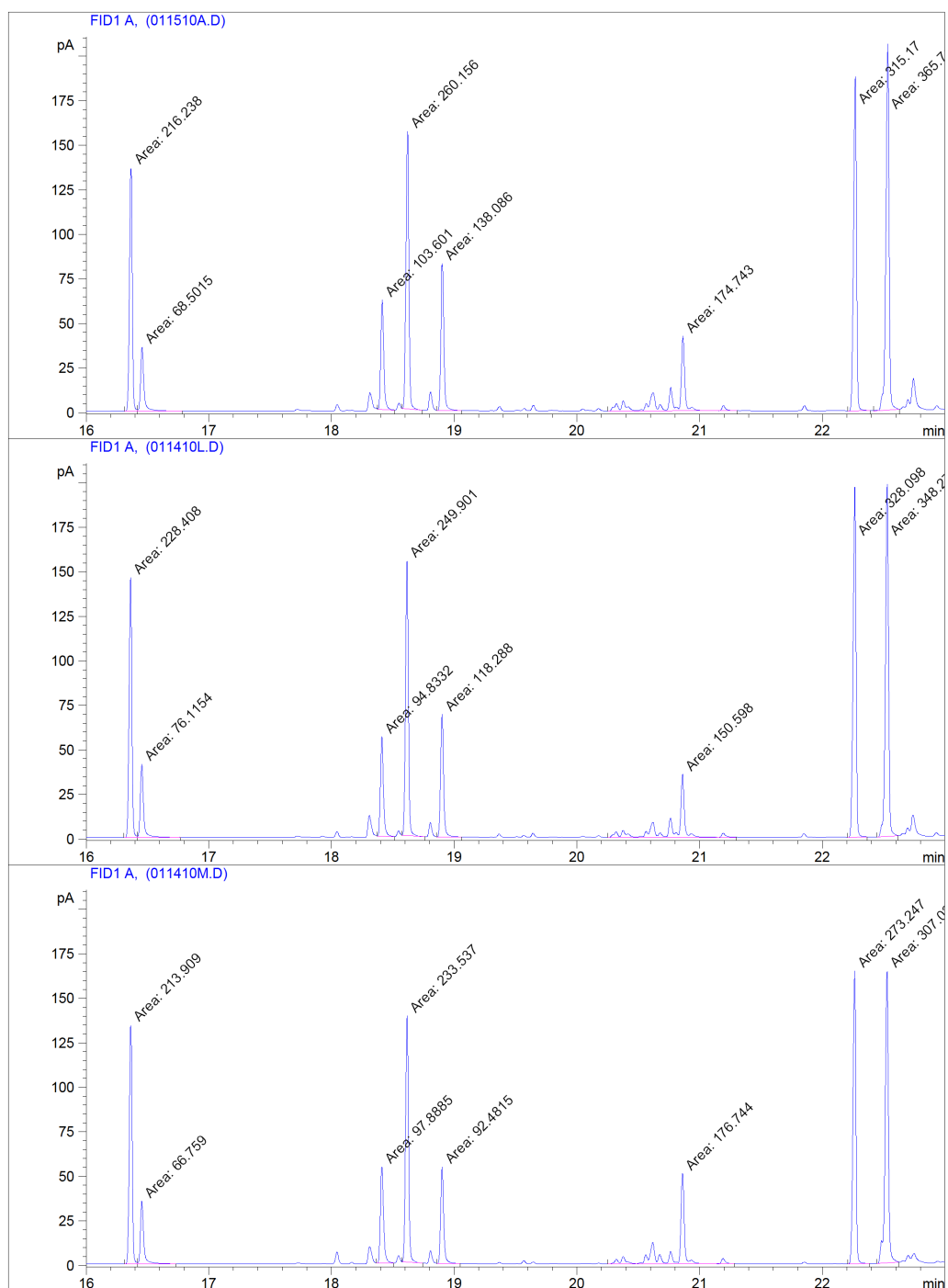Figure C.6: Day 9 ("stationary" phase) chromatograms for replete (top), +Urea,-Ni (middle), and+Urea,-Ni (bottom) sample

```
========================================================================
                           Integration Results
========================================================================

Signal 1: FID1 A,  (011510A.D)


Peak   Time    Type     Area        Height      Width    Start     End
  #    [min]           [pA*s]        [pA]        [min]    [min]    [min]
----|--------|----|-----------|------------|-------|--------|--------|
   1   16.365 MF    216.23825    136.80684   0.0263   16.311   16.417
   2   16.455 FM     68.50153     36.11587   0.0316   16.417   16.785
   3   18.412 MM    103.60082     61.65443   0.0280   18.374   18.515
   4   18.619 MM    260.15625    155.91162   0.0278   18.572   18.741
   5   18.899 MM    138.08643     82.50147   0.0279   18.857   19.058
   6   20.863 MM    174.74344     41.97244   0.0694   20.254   21.305
   7   22.269 MM    315.16953    187.43187   0.0280   22.208   22.392
   8   22.533 MM    365.71469    206.12054   0.0296   22.419   22.631


Signal 2: FID1 A,  (011410L.D)


Peak   Time    Type     Area        Height      Width    Start     End
  #    [min]           [pA*s]        [pA]        [min]    [min]    [min]
----|--------|----|-----------|------------|-------|--------|--------|
   1   16.361 MF    228.40773    146.11293   0.0261   16.309   16.416
   2   16.453 FM     76.11538     41.26066   0.0307   16.416   16.771
   3   18.408 MM     94.83318     55.81839   0.0283   18.373   18.510
   4   18.614 MM    249.90125    154.39546   0.0270   18.572   18.762
   5   18.900 MM    118.28757     69.00073   0.0286   18.857   19.058
   6   20.861 MM    150.59850     35.54401   0.0706   20.251   21.299
   7   22.264 MM    328.09753    197.52547   0.0277   22.206   22.365
   8   22.529 MM    348.27509    198.45345   0.0292   22.446   22.620


Signal 3: FID1 A,  (011410M.D)


Peak   Time    Type     Area        Height      Width    Start     End
  #    [min]           [pA*s]        [pA]        [min]    [min]    [min]
----|--------|----|-----------|------------|-------|--------|--------|
   1   16.361 MF    213.90874    134.61609   0.0265   16.310   16.418
   2   16.451 FM     66.75898     35.32895   0.0315   16.418   16.733
   3   18.408 MM     97.88852     54.15178   0.0301   18.366   18.507
   4   18.615 MM    233.53746    138.37599   0.0281   18.573   18.744
   5   18.900 MM     92.48151     54.24528   0.0284   18.860   19.049
   6   20.860 MM    176.74400     50.70209   0.0581   20.251   21.287
   7   22.263 MM    273.24747    164.54648   0.0277   22.209   22.388
   8   22.528 MM    307.02435    164.13512   0.0312   22.442   22.623


========================================================================
```

Table C.5: Day 9 ("stationary" phase) integration results for replete (top), +Urea,-Ni (middle), and+Urea,+Ni (bottom) samples

C.3 GC-FID methods supplement

C.3.1 Standards

Standards for the GC-FID analysis routinely included both internal (C19) and external (nC17) standards. Additional compounds were identified with standards purchased from Nu-Chek Prep (Elysian, MN) and Supelco (Bellefonte, PA). Elution order is displayed for the relevant standards (routine internal, external, and other external) and an example sample in Figure C.7, with relevant retention times in Table C.6. At high concentrations it is possible to lose resolution as peaks co-elute, consequently concentration was kept appropriately low (~50-100 ng/uL on column).

Standards were run for each instrument and column to insure correct peaks-compound relationships in the elution scheme. Two GC-FID were used throughout this thesis and the figures and tables in this section reflect results from an Agilent 5890 GC-FID.

Peak #	Approximate retention time (minutes)	Compound (nomenclature is a:b, where a = carbon length, b= double bonds)
1	16.43	17:0, nC17 Alkane (external standard)
2	16.48	14:0
3	18.4	16:2 (assumed)
4	18.6	16:1
5	18.9	16:0
6	20.78	18:2
7	20.89	18:1
8	21.22	18:0
9	22.3	C19 FAME (internal standard)
10	22.5	20:5 (EPA)

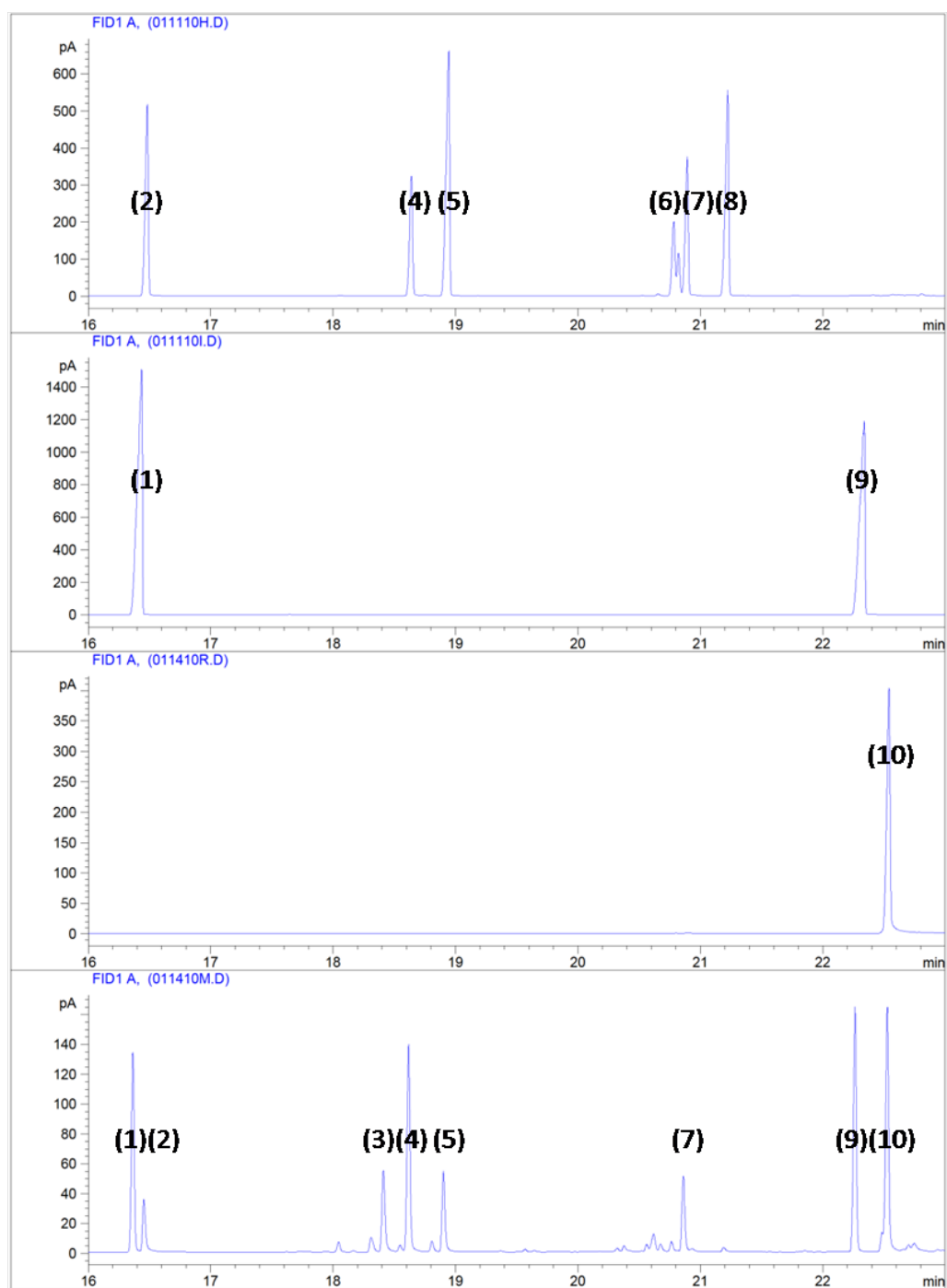Table C.6: Retention times for compounds identified in Figure C.7.

Figure C.7: Elution order of standards (top 3 frames), and an example sample (bottom frame).

C.3.2 FAEE to FAME conversion adjustment

The internal standard added is fatty acid ethyl ester (FAEE) (ethyl nonadecanoate) which through transmethylation is converted to fatty acid methyl ester (FAME). The FAEE has a retention time of ~22.9 minutes and was never observed in the final GC results assuring essentially 100% transmethylation efficacy. As a consequence of the transmethylation the FAME loses a carbon, hence the formula weight must be adjusted prior to using the FAME as an internal standard.

Correcting the internal standard for quantification requires that the FAEE mass added be multiplied by the factor 0.955 (a 4.49% reduction); this figure accounts for the formula weight proportion of FAME (312.53 g/mol) to FAEE (326.56 g/mol).

C.3.3 Internal response factor

The internal response factor (IRF) used in this work was determined with fresh standards on the same column and instrument used for all samples presented in Appendix Section C.2. For C19 as determined by nC17, the IRF = 0.985 and for all other calculations relating specific compounds to C19, an IRF of unity is taken since it is common practice to use this value for hydrocarbons in GC-FID analysis.

C.4 Algaculture methods

C.4.1 Protocol for $f/2$ media

The following tables and procedure is taken from *Guillard* [36], *Guillard and Ryther* [37] and has been used extensively by CCMP[1] where this information was sourced verbatim.

<div align="center">

$f/2$ **Medium**

(Guillard and Ryther 1962, Guillard 1975)

</div>

This is a common and widely used general enriched seawater medium designed for growing coastal marine algae, especially diatoms. The concentration of the original formulation, termed "f Medium" (Guillard and Ryther 1962), has been reduced by half.

To prepare, begin with 950 mL of filtered natural seawater and add the following components. The trace element and vitamin solutions are provided below. Bring the final volume to 1 liter with filtered natural seawater. If the alga to be grown does not require silica, then it is recommended that the silica be omitted because it enhances precipitation. Autoclave.

Component	Primary Stock Solution	Quantity	Molar Concentration in Final Medium
$FeCl_3$ $6H_2O$	---	3.15 g	1.17×10^{-5} M
Na_2EDTA $2H_2O$	---	4.36 g	1.17×10^{-5} M
$CuSO_4$ $5H_2O$	9.8 g/L dH_2O	1 mL	3.93×10^{-8} M
Na_2MoO_4 $2H_2O$	6.3 g/L dH_2O	1 mL	2.60×10^{-8} M
$ZnSO4$ $7H_2O$	22.0 g/L dH_2O	1 mL	7.65×10^{-8} M
$CoCl_2$ $6H_2O$	10.0 g/L dH_2O	1 mL	4.20×10^{-8} M
$MnCl_2$ $4H_2O$	180.0 g/L dH_2O	1 mL	9.10×10^{-7} M

<div align="center">

Table C.7: $f/2$ media constituents.

</div>

---

[1]https://ccmp.bigelow.org/node/58

<div align="center">$f/2$ **Trace Metal Solution**</div>

To prepare, begin with 950 mL of dH2O, add the components and bring final volume to 1 liter with dH2O. Autoclave. Note that the original medium (Guillard and Ryther 1962) used ferric sequestrene; we have substituted Na2EDTA • 2H2O and FeCl3 • 6 H2O.

Component	Stock Solution	Quantity	Molar Concentration in Final Medium
$NaNO_3$	75 g/L dH_2O	1 mL	8.82×10^{-4} M
$NaH_2PO_4\ H_2O$	5 g/L dH_2O	1 mL	3.62×10^{-5} M
$Na_2SiO_3\ 9H_2O$	30 g/L dH_2O	1 mL	1.06×10^{-4} M
trace metal solution	(see recipe below)	1 mL	---
vitamin solution	(see recipe below)	0.5 mL	---

<div align="center">Table C.8: $f/2$ trace metal solution constituents.</div>

<div align="center">$f/2$ **Vitamin Solution**</div>

First, prepare primary stock solutions. To prepare final vitamin solution, begin with 950 mL of dH2O, dissolve the thiamine, add 1 mL of the primary stocks and bring final volume to 1 liter with dH2O. Filter sterilize. Store in refrigerator or freezer.

Component	Primary Stock Solution	Quantity	Molar Concentration in Final Medium
thiamine HCl (vit. B_1)	---	200 mg	2.96×10^{-7} M
biotin (vit. H)	1.0 g/L dH_2O	1 mL	2.05×10^{-9} M
cyanocobalamin (vit. B_{12})	1.0 g/L dH_2O	1 mL	3.69×10^{-10} M

<div align="center">Table C.9: $f/2$ vitamin solution constituents.</div>

C.4.2   Sterilization protocols

For small volume (< 1 L) cultures, microwave sterilization or autoclave was used. Any cultures over 1 L were sterilized (both media and culture) with chlorine. Regular household bleach (6%, or 0.87 M sodium hypochlorite) was added at 0.5 mL per L of culture medium. Following an 8-12 hour sterilization period (including gentle mixing by air bubbling), Sodium Thiosulfate (1 Molar stock solution) was added at 0.125 mL per L of culture media. Inoculation can be done within minutes of the thiosulfate reduction step.

Appendix D

Additional studies

D.1 Solvent extraction comparisons

Different extraction solvents have varying rates of efficacy. While hexane is inexpensive and commonly used for lipid extractions, DCM/MeOH recovers more constituents (pigments for example). As an additional study I briefly compared extractions with each (1) Hexane and (2) DCM/MeOH. Normalizing for quantity of biomass processed the (TLE mass as percent of dry-weight biomass processed) it was found that with (1) %TLE = 2-4, whereas with (2) %TLE = 12. Consequently, from 3-6 times more mass is extracted with (2) than (1). This difference is evident in chromatograms from the same samples. In Figure D.1, the dominant peaks at retention times of circa 13 and 19 are for external and internal standards respectively; between the standards it is evident without quantification that more variety of compounds were extracted with DCM/MeOH (lower) than Hexane (upper).
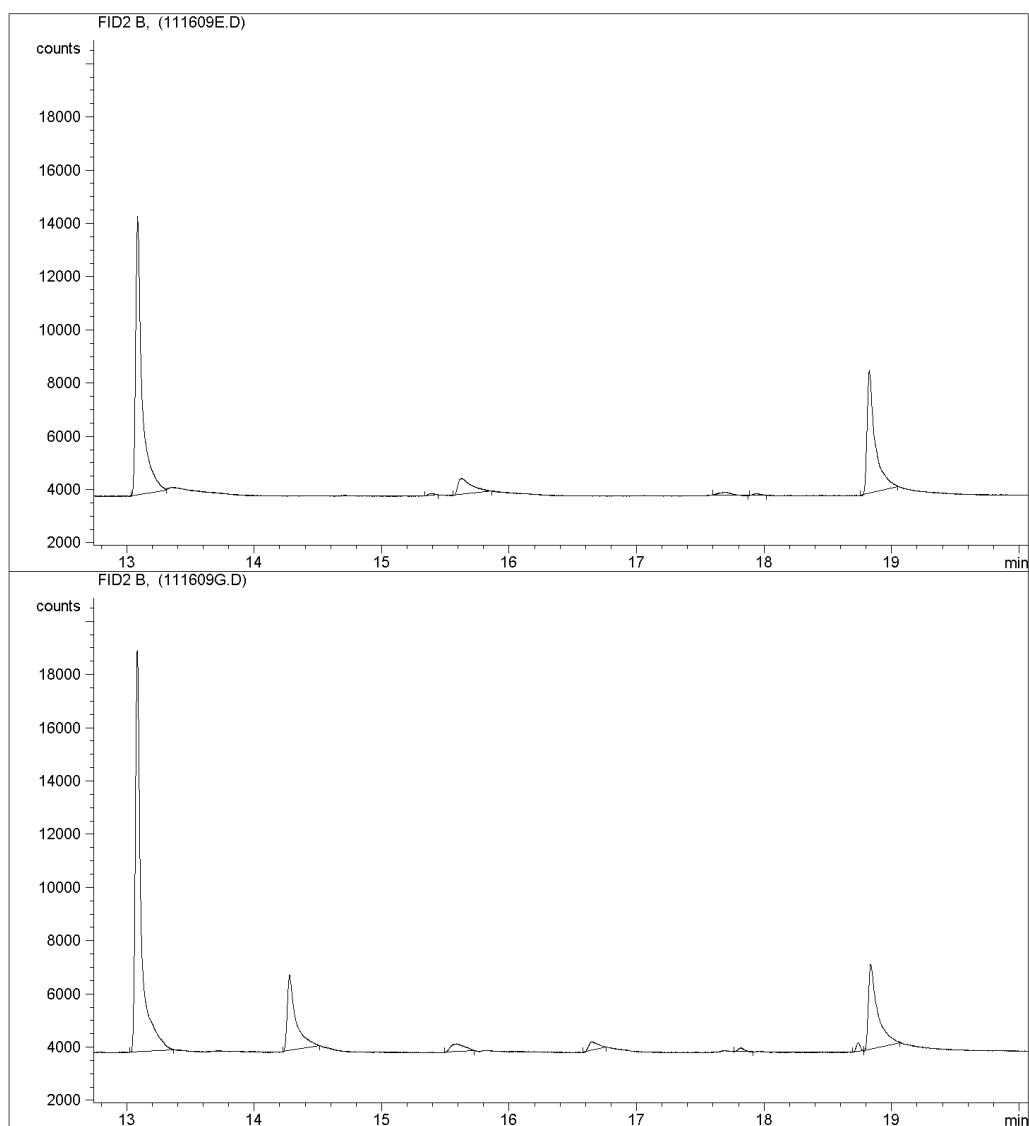
Figure D.1: Chromatograms comparing Hexane and DCM/MeOH extractions

D.2 Novel antarctic cyanobacteria

This section focuses on results of a screen for interesting novel microbes that might be used for bioproduction, particularly in relatively cold culturing climates. Specifically, three cyanobacterial assemblages collected from Antarctic fresh-water lakes were cultured in BG11 medium. The biomass from these samples was prepared as detailed in Section 3.2.3. Results from the GC-FID

quantification are shown in Figure D.2, along with transesterified canola oil for comparison.
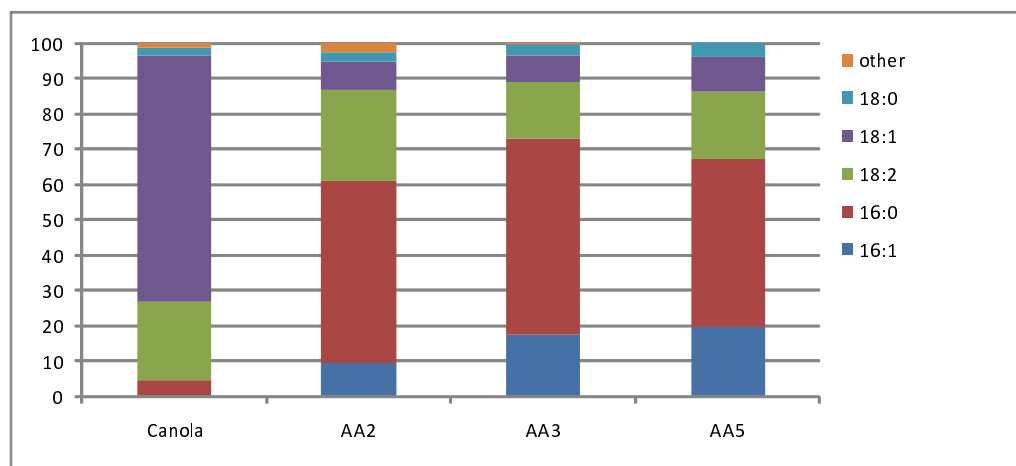
Figure D.2: Antarctic cyanobacteria FAMEs distribution for three cyanobacterial assemblages (AA- 2, 3, 5) compared to a reference of transesterified canola oil (far left) for comparison.

Growth curves for these cyanobacteria are difficult to prepare as a result of their tendency to grow in colonial form. Also, to simulate their natural environment the results here are from cultures maintained at 4ºC. These cultures and prospects of such novel microbes for bioproduction in cold climates is in demand – future work may better qualify these and other microalgae by detailed assessment of lipid productivity and lipid quality as characterized by methods similar to this thesis.

TLE with DCM/MeOH extraction was comparatively low (13-18% by dry weight) for the cyanobacteria discussed here (relative to both *Isochrysis*, and *Phaeodactylum*).

D.3   State and national feasibility study (Massachusetts & USA)

As a preface to this thesis one subject matter was to look regionally throughout the United States based on available solar energy and prepare a "back-of-the-envelope" calculation for the potential of biofuels (namely from microalgae) to replace our current petroleum demand in the surface transportation sector. This effort is more of a general thought experiment, and while it should not be used for substantial evaluation, it can complement existing estimates as an independent and un-biased analysis.

The objective was to estimate if based on limited pilot scale productivity estimates the US could sustain current transport fuel needs with fuel from a microalgae based bioproduction system, and if so, what percent of existing farm land would be required. Farm-land was selected as a reference and it should not imply that arable land would be required for such a scheme (in fact it would be ideally discouraged, thus reserving quality agriculture land for food crops).

The main estimate for conversion efficiency on which the entire calculation is based comes from *Huntley and Redalje* [44], after adjusting for hypothetical energy inputs (10%) and incomplete conversion to biodiesel (assumed 80% efficacy based on *Chisti* [16]). The conversion efficiency used was slightly below 0.5% (significantly lower than the theoretical value of *Bolton* [10], <13%). In reality the value will likely fall between these.

Current data for inputs included state-by-state data and sources as follows:

Agriculture land use U.S. Department of Agriculture[1]

Total non-water area Census 2000 Summary File[2]

Fuel by state Department of Transportation[3]

Solar radiation resource National Renewable Energy Labs[4]

Calculations were performed in Microsoft Excel, though details are not included here, they may be supplied upon request from the author (tyler.goepfert@uni-oldenburg.de).

---

[1]http://usda.mannlib.cornell.edu/MannUsda/viewDocumentInfo.do?documentID=1259
[2]http://factfinder.census.gov/servlet/DCGeoSelectServlet?ds_name=DEC_2000_SF1_U
[3]http://www.fhwa.dot.gov/policyinformation/pubs/pl08021/excel/Fig5_2.xls
[4]http://rredc.nrel.gov/solar/old_data/nsrdb/redbook/atlas/

The result showed that while the state of MA could not meet its own needs for transport, the USA on the whole could do so with an equivalent of 1.6 times current agriculture land. This result prompted a quick sensitivity analysis of the conversion efficiency and resulting fuel production potential and land requirements relative to existing agriculture land for the nation as a whole. This analysis is summarized in Figure D.3.
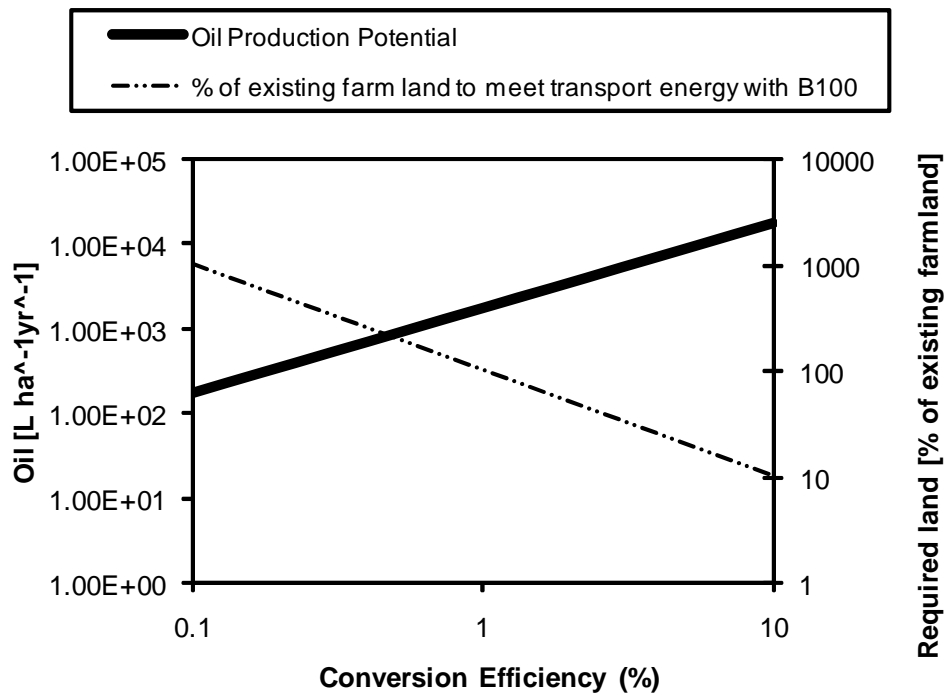

Figure D.3: Sensitivity analysis on biomass solar energy conversion efficiency and resulting fuel production and land use estimates.

These calculations provide a very rough estimate on what is believed to be a lower-bound on potential as a function of solar energy conversion efficacy (assuming biodiesel [B100] production).

Appendix E

Sundries

E.1   Further background and informal discussion

Theoretical solar conversion potentials

In the late 1970s, inspired by evidence of peak oil, *Bolton and Hall* [11] discussed the merit and theoretical limits of solar fuel production and summarized that photosynthesis may in fact be the optimal target pathway for such a goal. *Bolton* [10]states in reference to microbial photosynthesis that:

> *"Such a process would have a decided advantage over the solar generation of electricity in that conversion and storage are carried out in the same process."*

Shockley (now famous in namesake for the Shockley diode equation in the PV industry), and others developed theoretical maximum conversion efficiency bounds of ~31% in AM0 sunlight conditions [97]. Later further generalized photochemical solar energy conversion, and even Plank and Kirchhoff based limits corroborated the 31% ideal boundary as noted by *Bolton et al.* [12].

While ideal maximum conversion efficiency from sunlight to stored chemical energy in carbohydrates is ~13.3% (comparable to modern-day thin-film Photovoltaic technology), the "net" efficiency after dark and photorespiration considerations is only ~5.6% [11]. Of great significance however is that this conversion efficiency is into stored energy not instantaneous conversions as are unfortunately often compared with the potential from photo-bio conversion systems.

Meeting fuel demand

The general public often only consider electricity when discussing energy and power; however, fuels (especially in the transportation sector) are an especially important topic. In the US, nearly a third of all primary energy is dedicated to transportation with petroleum contributing 95% of the fuel supply in this sector [4]. What's more, there is evidence that our growing demand in the transportation sector may be larger than previously estimated from standard top-down methodology. Over a recent 10 year period it was shown that while IEA data show a 1.7% growth rate, an alternative bottom-up approach revealed up to 12% growth for the same period [119] (the difference being ~40 vs 6 year doubling-times respectively). Consequently it is possible that our ability to continue fueling growth will be compromised if such growth estimations may be significantly different from reality.

Green chemistry

Commercial and current fossil-based industries favor inherently unsustainable (often toxic, polluting, and disruptive) approaches. The scale of fossil evolution is emphasized by *Pokhodenko and Pavlishchuk* [78]:

> *"Total growth in production for petroleum refining and the basic and fine chemical synthesis industry has surpassed the volumes of chemical production in all previous human history by several orders of magnitude.... Of course, such rapid growth in chemical production entails sharp growth in the amount of wastes that can endanger the environment."*

A growing response to the above concern is green chemistry which addresses the root of fossil-based energy problems rather than mitigation strategies.

Algal bio-energy focus is fundamentally natural in comparison with most other energy solutions. While natural systems may not always have high efficiency we must consider externalities (in light of modern concern for environmental quality and biodiversity as related to climate change and natural stability).

Distinction between algae/microalgae and microbes

Microbes or micro-organisms are a broad class of living cells characterized by their small (hence, micro) size. Microalgae are uniquely photosynthesizing microbes further defined for the purposes of this study as was previously defined by *Wang et al.* [110]:

> *"...[M]microalgae [are] all unicellular and simple multi-cellular photosynthetic microorganisms, including both prokaryotic microalgae, i.e., Cyanobacteria (Cyanophyceae) and eukaryotic microalgae, e.g., green algae (Chlorophyta) and diatoms (Bacillariophyta)."*

The cyanobacteria tend not to be lipid accumulators, and are less optimal for bio-oil, but do however produce other useful compounds and perhaps can be coupled in a mutualistic way on account of their ability to fix atmospheric nitrogen (they are effectively the ligumes of the sea). Cyanobacteria are the only group of organisms that are able to reduce nitrogen and carbon in aerobic conditions. For fuels reduced carbon is the desired species, and in a closed system if an organism can also reduce nitrogen itself, that is advantageous.

E.2 Fuel potentials and conversion techniques

Cellulosic ethanol

In the early 1990s ethanol gained wide support as a prospective future renewable fuel substitute to fossil fuels [60]. Indeed ethanol production has seen significant development, albeit with significant recent concern over its degree of appropriateness [28]. Further, it has been argued that sugar cane is the best way to produce bioethanol from both the economical and the environmental point of view, including GHG mitigation through the use of ethanol as a gasoline substitute .[88]. The debate in cellulosic biofuels appears to run deep with agro-industrial and political dimensions not soon to be resolved.

Gasification potential

Wu et al. [113] summarize potential for gasification:

> *"E. huxleyi is a nice experimental system for studies on the origin of marine petroleum and natural gas. This species is also suggested as promising biomass in production of renewable fuels by means of pyrolysis."* [114]

Balat et al. [7] presents an excellent contemporary overview of this technology noting that currently the main purpose of biomass gasification is the production of low- or medium heating value gas for internal combustion engines and/or

power production. *Balat et al.* [7] further argue that a more effective use of the biomass resource is a coupling of bio-syngas (from gasification) with Fischer-Tropsch Synthesis (FTS) to prepare an excellent No. 2 Diesel replacement having the added advantage of no aromatics or sulfur compounds.

Direct Alcohol production

In early 2008 news of synthetic biologist James Liao's efforts at University of California, Los Angeles highlighted progress with photosynthetic bacteria toward directly making isobutanol [6].

> *"Liao and his co-authors described how they engineered E. coli to produce isobutanol, a longer chain alcohol than ethanol. That increased chain length gives isobutanol a more energetic punch per liter and enables it to be separated from water more easily, Liao says. The molecule can also easily be converted to fuels that can be blended with gasoline as well as transformed into other commodity chemicals."[93]*

Hydrogen production

Hydrogen production from cellulosic material is yet another potential pathway for fuel generation, however it relies heavily on yet to be refined (hyper)thermophilic enzymes in a simple one-pot production method [115]. Alternatively direct bio-photolysis or "photobiological hydrogen production" can be employed as proposed by NREL investigators:

> *"...[H]ydrogenases in the green alga, Chlamydomonas reinhardtii, are being engineered to remove the detrimental oxygen-sensitivity property. The ultimate goal of this work is to develop a water-splitting process that will result in a commercial hydrogen-production system that is cost effective, scalable to large production, non-polluting, and self-sustaining."[1]*

Researchers at UC Berkeley are working with *Chlamydomonas* deprived of sulfur while exposed to light which results in hydrogenase production and spurring release of H_2. *Hemschemeier et al.* [39] provides some of the most recent and interesting synthesis of work done using *C. reinhardtii* for direct hydrogen production.

---

[1]*http://www.nrel.gov/basic_sciences/technology.cfm/tech=16*

Advanced hybrid schemes

Hydrogen, gasification, hydrothermal carbonization, and fuel cell technology are some of the hottest topics under current investigation with respect to renewable energy. Perhaps an obvious prospect is the coupling of technologies, for example to use of the spent bio-mass residuals from one process toward one or more of the following:

- Anaerobic biogas digestion (ABD)

- Gasification

- Fast Pyrolysis toward liquid fuel production

- Hydrothermal carbonization, and Hydrothermal electrolysis (of glycerol for example: [118])

- Use suitable biomass toward direct carbon fuel cell

E.3   Challenges within microalgal biofuels

Scaling up

A chemostat steady-state model can be reduced to a relatively simple system described by equation E.1.

$$\mu = f/V \qquad\qquad (E.1)$$

where,

$\mu =$ specific growth rate

f = bulk media flow rate

V = reactor volume

and can be rearranged for f defining the appropriate cell dilution (or harvest) rate at steady state. Immediately apparent here is the benefit of a large system for bulk production, economies of scale, and a hope for future biofuel substitution in place of environmentally worrisome fossil fuels.

In nature, as well as in any conceivable large-scale production system, the notion of steady state is impractical because of the multitude of stochastic parameters (seasonal and diurnal light variability, nutrient regime changes, etc). Consequently a quasi-steady-state model is often assumed leading to in imperfect, but still reasonable predictability in production. It would seem that larger systems are more resilient, though conceivably more complex from a maintenance/management perspective.

To overcome scaling problems one approach is to expand with modular units which can be isolated during maintenance or trouble-shooting. When a culture is in exponential growth it must be continuously supplied with all necessary nutrients which may become a great challenge in commercial production scale – one work-around to modulate growth would be shading and/or temperature regulation. Alternatively a batch system could be employed, although the consensus seems to be that for large scale commercial production a continuous (or at least nearly continuous) strategy must be employed.

Competition

With the global $1 trillion per year market for energy, it is thought there is plenty of room for many players. Echoing the sentiment from throughout the biofuel competition, Stephen Mayfield, a cell biologist at the Scripps Research Institute in San Diego, California, claims the more biofuels players, the better. "We will use every molecule of renewable energy we can get." [94].

Even in cool mid-latitudes there is progress in species selection and growing biodiesel production with successful partnerships that have recently been publicized showing the importance of cross-disciplinary interaction and public-private partnerships around the world [72].

Competition is not always contributing in a positive way; when a shrimp farm or other aquaculture business spins their existing systems to solicit funds from public and private investors it only draws resources away from genuine investigation and technology improvement – moreover when the off-shoot fails it brings a bad name to an industry just getting off the ground.

The water problem

An astute cyber-citizen recently posted:

> *"Before you make algae into fuel for cars, you have to dry it.*
> *Cars can't burn water. It takes more energy to dry the algae than*

> *you can recoup from the biomass. This has been researched decades ago. The conclusion was (and will be again) that it won't work because of the high water content in algae."*[2]

So, what is the truth of this matter, the current state of technology, and reason for sustained optimism that surrounds this topic.

In the case of Paul Woods (CEO of Alganol), it is ethanol which solves the de-watering problem. Alganol's technology has been licensed to BioFields of Mexico and involves no de-watering, crushing, or processing as it makes use of bio-ethanol production and it's inherent volatility for separation from the bio-reactor bulk media[21].

Alternatively, solvent extractions can be employed. And more recently novel methods such as pulsed electric field (PEF) technology are being investigated for recovery of oil from the bulk algaculture solution. Dewatering is a well-known problem and one being actively addressed as reflected in a review by *Uduman et al.* [106].

Media and research hype

Even scientific literature is prone to a form of hype, that is a proven bias towards positive results in peer reviewed journals [48]. With care and guarded optimism it seems appropriate to continue pursuing the algae to energy grail.

E.4   Internet resources

The following links have been screened for reliable content and are considered to be of reputable quality within the context of introductory references for microalgal biofuels technology.

General interest and institution urls

http://www.nrel.gov/biomass/proj_microalgal_biofuels.html

http://www.algalbiomass.org/

https://ccmp.bigelow.org/

---

[2]http://www.bionomicfuel.com/scientists-confirm-algae-is-the-most-effective-alternative-energy-source/

Recent popular media urls

http://www.wired.com/wiredscience/2009/12/the-lost-decade-of-algal-biofuel/

http://www.triplepundit.com/2009/03/algae-biofuel-hype-hope-and-promise/

E.5 Miscellaneous points and claims for consideration

- Microalgae can capture sunlight 20-40 times more efficiently than plants, and unlike corn- or soy-based feedstocks, they do not create a "food or fuel" dilemma[3].

- The reality is that algae is not a panacea or a complete solution. Dr. Benemann of Benemann Associates drove the point home: "(We) can't replace oil with algae – there is too much hype and hope."[4]

- We must seek continued basic understanding of the molecular biology in underlying topics such as the fatty-acid biosynthesis pathways and acyl-transferases involved in glycerolipid synthesis [32]

- The contentious GMO topic (and to it's extreme, synthetic genomics who may aim to design and patent life from the molecular level)... a variety of perspectives are discussed in the following references [109, 34]

---

[3] http://www.renewableenergyworld.com/rea/news/article/2009/09/algae-biofuels-from-pond-scum-to-jet-fuel

[4] http://www.triplepundit.com/2009/03/algae-biofuel-hype-hope-and-promise/

E.6   Biographical summary

Tyler Jay Goepfert was born in Williamsville, NY, USA. After attending Cornell University (1999-2003) completing a B.S. in Engineering he worked for 3 years at the Woods Hole Oceanographic Institution (WHOI) where he investigated topics in trace metal biogeochemistry (2004-2007). Following this work at WHOI he worked for a year at the University of Southern California (USC) as lab manager and research assistant in the Moffett Trace-metal laboratories (2007-2008). Most recently Tyler studied at the University of Oldenburg, Germany (Postgraduate Programme Renewable Energy). M.Sc. work during studies at Oldenburg are presented in this thesis (2008-2010).

Tyler can be contacted by email at: tyler.goepfert@uni-oldenburg.de

Index